CrossMark

REVIEW

*This section of Journal of Materials Research is reserved for papers that are reviews of literature in a given area.*

# Fiber-reinforced magneto-polymer matrix composites (FR–MPMCs)—A review

Muhammad Musaddique Ali Rafique[a)] and Everson Kandare
*School of Engineering [Aerospace, Mechanical and Manufacturing], College of Science, Engineering and Health, RMIT University, Bundoora, VIC 3083, Australia*

Stephan Sprenger
*Business Line Interface and Performance, Evonik Nutrition & Care GmbH, Geesthacht 21502, Germany*

(Received 10 July 2016; accepted 6 February 2017)

Magneto polymer matrix composites (MPMC) is a new class of magnetic polymer materials which are being developed and under investigation as potential materials for tomorrow's aircraft structures. It encompasses magnetic, particulate strengthening (dispersion strengthening) as well as fiber reinforcement/strengthening characteristics which are sought out to be utilized toward making efficient future aerospace composite materials. Various types of ferrites including barium, cobalt, iron, and strontium were explored for being used in making new composites. Here a comprehensive review of the synthesis, structure, properties, thermodynamics, surface chemistry, and phase transformations of individual ferrites and clusters of ferrites as fillers is presented. In particular a discussion about the rational control of the mechanical, physical, thermal, electrical, and magnetic properties of magneto polymer matrix composites through surface functionalization, modification, emulsification/compounding/blending, heat treatment (phase transformation and separation), and control of processing conditions (temperature, pressure and geometry of mold) is provided. These smart materials have a wide range of potential applications in medicine, drug delivery, bio imaging, bio marking, tissue engineering, electromagnetic interference (EMI) and electromagnetic force (EMF) shielding, and as competent materials for aerospace structural applications.

## I. INTRODUCTION

Magnetism was discovered as early as 600 B.C when loadstone [a mineral of iron and oxygen (magnetite)] was discovered but it was until the 20th century that scientists have begun to understand it and make use of its benefits by developing technologies based on it.[1,2] Magnetic particles (ferrites) have been tested for use in polymeric composites [also known as ferrite polymer composites (FPC) or ferrite particulate reinforced composites (FPRC)] as far as 60 years ago.[3–7] Magnetic (inorganic) particles have been extensively studied and used in both already conducting and nonconducting polymer matrices as magnetic sensors,[8,9] magnetic recording media,[10] soft magnetic materials,[11,12] EMF shielding,[13] electromagnetic wave (radiation) absorbing media,[14] EMI shielding,[15] biomedical markers,[16,17] vibration damping media,[18,19] wireless radio communication systems and sensors in various technological applications. However, their use in "aerospace structures" is limited by the fact that they are very selective and cause problems in fluidity, manufacturing, mechanical strength and corrosion, if added beyond a certain limit which is very low for magnetic detection.[20] Some further issues which might be encountered during the use of magnetic particles in polymer matrices and limit their applications are

(i) **Magnetic confinement**: Their ability to be deformed (stretching, bending, and rotation) under the application of a magnetic field. This is found in conjunction to, and is in contradiction of absolute requirement of magnetic field for causing alignment in magnetic particles mixed in resins to achieve magnetic anisotropy, directional properties and preferential magnetic ordering (domain orientation) without which, a material will only show very poor or no response to an externally applied magnetic field. The adverse effects of confinement are that it is difficult to handle the material in other applications and service conditions where it comes in contact with ferromagnetic (active or passive) components.

(ii) **Magnetic guidance**:

(a) **Interaction with air bubbles**: During laminate formation, magnetic particles [especially in non-reacted/unstirred condition—(when they retain their identity)] can interact with gas molecules and bubbles and help avoid their formation and growth. This can be used to

Contributing Editor: Michael E. McHenry
[a)]Address all correspondence to this author.
e-mail: s3469212@student.rmit.edu.au, ali.rafique@hotmail.com
DOI: 10.1557/jmr.2017.63

 © Materials Research Society 2017

https://doi.org/10.1557/jmr.2017.63 Published online by Cambridge University Press

advantage by controlling the processing conditions such that these can diminish the effect of bubble formation. What is required is that the process should be controlled in such a way that each time a bubble tends to form in the matrix; a magnetic particle should interact with it, break it and thus retard its formation. This can be fine-tuned to form excellent porosity free laminates.[21,22] This however, can turn toward exhibiting detrimental effects if particles are added and present in matrix beyond a certain limit.

(b) **Self-healing**: Studies have been carried out to incorporate magnetic particles in a matrix and use them as healing medium by heating the composite later on by resistive heating. This idea utilizes induction heating as source of heat energy which is caused by hindrance to motion of magnetic particles in polymer matrix thus these get heated by friction against polymer molecular chains, generating heat, which is used to fabricate structures which can self-heal upon exposure to induction heating after damage detection or onset.[23–25] This can also be used to produce thermal energy activated shape memory effect (SME).

(c) **Bio marking and drug delivery**: Magnetic particles can be used to carry certain drugs to certain areas of body/cell preferentially as compared to other areas owing to their response to magnetic field. This can be used to attack certain defective cells in a body. This can also be used to induce drugs/mechanisms which can damage/kill certain affected/defective cells (cancer treatment). This field however, needs further research.[16,17,26]

(d) **Joule heating**: This is more prominent in case of carbon fiber reinforced plastics (CFRP) and is mainly due to resistance offered by strong carbon fibers to motion of magnetic particles inside the matrix when subjected to magnetic field. The motion, though minute and intrinsic, is enough to cause heating in layers to initiate loss of bonding at fiber/matrix interface and complete delamination in case of severe heating.

(e) **Magnetic entanglement**: Aircrafts generate huge amounts of electromagnetic fields upon engine start-ups. Similar effects are also present in and around airports, test ranges, open pit, and excavated mines, oilfields, radio telescopes and other high energy devices which often come in contact with airplanes. This has severe effect on magnetic confinement resulting in entanglement in already magnetic polymer matrix composites.[39]

(f) **Magneto–rheological effect**: Preferential ordering and alignment of magnetic nanoparticles under the action of externally applied magnetic field can cause orientation and pearl chain structure development in polymer blends. This phenomenon is called magneto rheological effect (MRE).[27–33]

(g) **Vibration damping**: A similar methodology can be used to control mechanisms and procedures in which fine tuning of magnetic particles can be used to devise vibration damping mechanism. This is especially useful in civil engineering; FMCG and automotive industry where there is need to have components with self-vibration damping ability. This can effectively be used toward non-destructive testing of CFRP car wheels—a method currently actively under investigation as potential method for NDT of composite wheels.[144]

(iii) **Filtration and preferential screening**: Excess percentage of nanoparticles can result in preferential screening and filtration by a fiber mat and supporting gauze during processing resulting in coagulated areas in pipes near the entrance, conglomerates of particles, preferential screening, and in worst case scenarios, complete system blockage with no resin infusion at all.

It is further advantageous if the matrix could be conducting with a damage mechanism which is atom/ion to atom/ion transfer. These problems and others alike can only be overcome by the use of superior magnetic particles which not only are small in size but very highly responsive toward magnetic fields. Other properties of interest are (i) ease and relative simplicity in synthesis (individual chemical synthesis) (ii) cheap and ready availability (iii) ease in further processing into composites (iv) ease, reduction or elimination of post processing steps and (v) with growing awareness and cautiousness toward environment, recyclability. Very recently, efforts have been made to address these challenges. The present study is focused on condensing these works into one comprehensive review which will encompass all the information and details described aimed at proposing magnetic nanoparticle polymer matrix composites as materials of the future.

## A. Classification of magnetic polymers

In general magnetic polymers can be classified into following categories as shown below (Fig. 1).

During the course of this review, our discussion will remain focused around magnetic plastics or magnetic rigid polymers. It should be noted that highly elastic composites are the class of plastics which have their $T_g$ near or below room temperature thus they exist as rubbery phase or rubber emulsions at room temperature. On the other hand, solid or rigid shape in case of rigid plastics is not due to $T_g$ or addition of fillers but it is due to intrinsic nature (size, type, and entanglement) of molecular chains that are arranged in such a fashion that a solid/rigid polymer results. That's why they are called intrinsic magnetic polymers as well. The effect of extrinsic factors such as molecular weight, self-curability, degree of cross linking, prior history, fillers [type, size, size distribution, nature (dispersed or attached)] and exposure conditions all play their part toward toughening and thus rigidity of polymers. These materials are also called ferrite reinforced composites (FRC), particulate ferrite reinforced

https://doi.org/10.1557/jmr.2017.63 Published online by Cambridge University Press

composites (PFRC) or in some cases simply particulate reinforced composites (PRC).

Some reports[21,22,34–57] appeared in late nineties—late half of first decade of 21st century but still they were limited to the use of particulate fillers (specially soft ferrites) in composites and their chemical characterization to check the effect of dispersity, attachment, weight percentage but very little effort has been made to check the effect of ferrite (hard) particulate reinforced composite (FPRC) toward making thick glass fiber reinforced composite (GFRP) plies and laminates with different orientation, stacking sequence and check their effectiveness toward magnetic response as established damage detection and assessment technique (magnetic flux leakage) for detection of manufacturing defects in aerospace and automobile structures—which is aimed as future potential arena of research.

## B. Ferrites

Ferrites are known for their magnetic effect as early as 1954.[6] These are the main materials (oxides) responsible for magnetic effect in magneto polymer matrix composites (MPMCs). Gabriel and co-workers[39] proposed a model explaining the mechanism by which magnetism evolve in magneto polymer matrix composites. They explained the generation and evolution of magnetism in magneto polymer composite on the basis of mechano-quantic theory in which paramagnetism of oxygen (at tetrahedral or octahedral sites in ferrite) is explained by means of molecular orbital method (MOM). The diagram in Fig. 2 is utilized to explain paramagnetic behavior of oxygen molecule.

It is clear that there are two unbound electrons in the antibonding orbitals $\pi^*_{2px}$ and $\pi^*_{2py}$ and according to Hund rule antibonding orbitals having the same energy are populated by one and only one electron at one time. This accounts for paramagnetic behavior of oxygen in the presence of external magnetic field. Another theory accounts for unequal distribution of cations and anions in Ferrite unit cell at tetrahedral and octahedral sites which even after cancellation bear a net positive effect and thus become a source of responsive behavior in an applied external magnetic field.[7] There are two types of ferrites.

## C. Soft ferrites

Ferrites (magnetic materials) which become magnetic upon application of magnetic field and returns back to their natural demagnetized state after removal of magnetic field are called "soft ferrites". An example of these ferrites is NiZn, MnZn. Out of these, NiZn ferrites and its derivatives have low to high Curie temperature ($T_C$) (130–500 °C) which makes them very close to hard ferrites. In fact, in case of application of strong magnetic field and/or severe plastic deformation (mechanical working), they actually can retain their permanent magnetic character even after removal of applied magnetic field. On the other hand, MnZn class of ferrites (MnZn and its derivatives) have low Curie temperature ($T_C$) (150–200 °C) which make them so called "perfect soft" magnetic materials as they do not retain magnetism upon removal of applied magnetic field and comes back to their demagnetization state.

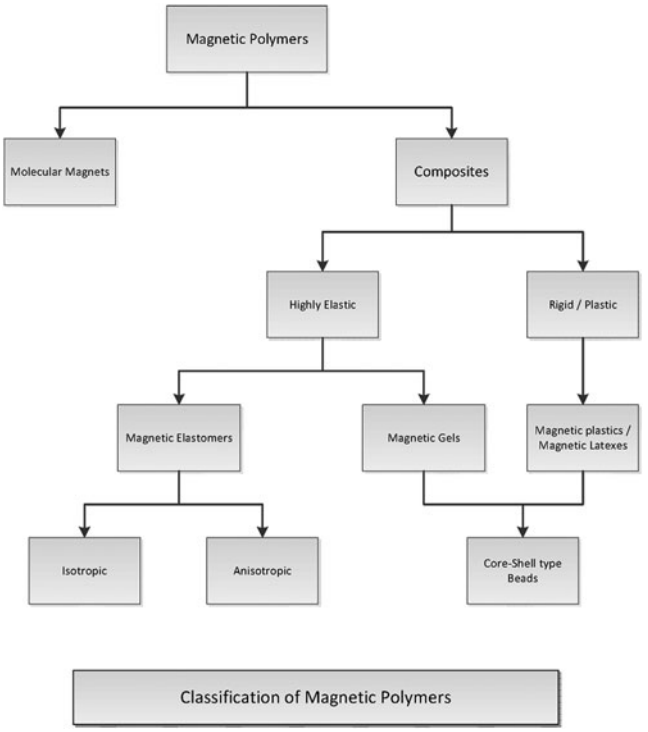



FIG. 1. Classification of magnetic polymers.

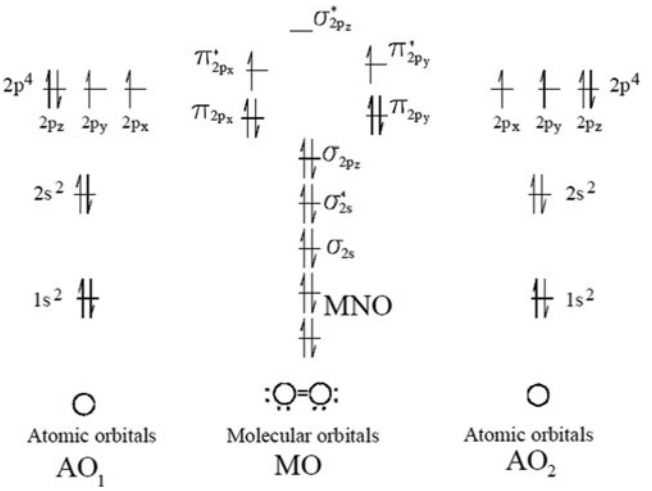



FIG. 2. Schematic representation of chemical bonds in $O_{2x}$ molecule, using MOM.[39]

https://doi.org/10.1557/jmr.2017.63 Published online by Cambridge University Press

### D. Hard ferrites

Ferrites which do not come back to their demagnetized state but retains their magnetism even on removal of applied field are called "hard ferrites". For example, barium ferrites, strontium ferrites, and cobalt ferrites. All these ferrites have their magnetic domains aligned and/or unaligned with a net positive magnetic effect in the direction of magnetic field in such a way that upon removal of applied field the "net positive effect" incurred in sample stays there indefinitely and becomes the source of the their permanent magnetic nature (Table I).

Another table below compares the salient features and properties of hard and soft ferrites describing each's merits and disadvantages (Table II).

### E. Selection of ferrites

The selection of ferrites is a critical step during magneto polymer matrix composite (MPMC) manufacturing and must be carried out carefully in conjunction with other properties of the system. A bad selection can result in damage or in worst case complete failure/non-functioning of system resulting in capital, energy and human life loss. Three of the most important criteria for selection of polymers are glass transition temperature ($T_g$) of the polymer matrix (before and after curing), cure temperature of the polymer resin matrix, and Curie temperature ($T_C$) of the ferrite. A ferrite cannot only be selected on its own properties as it has to be used in polymer matrix so the properties of the whole system must be taken into account before proceeding any further. Although there

TABLE I. Common ferrites and their raw materials.

| Sr. No. | Ferrite | Raw material | Reference |
|---|---|---|---|
| | | $M^{2+}$ precursor / $Fe^{3+}$ precursor | |
| 1 | $Zn_{0.2}Mn_{0.8}Fe_2O_4$ (ZMFO) | $ZnCl_2$ (98%), $MnCl_2$ (99%) / $FeCl_3{\cdot}6H_2O$ (99%) | 8 |
| | $CoO{\cdot}Fe_2O_3$ | $CoCl_2{\cdot}6H_2O$ (98%) / $FeCl_3{\cdot}6H_2O$ (99%) | |
| | $Fe_3O_4$ | $FeCl_2{\cdot}4H_2O$ (99%) / $FeCl_3{\cdot}6H_2O$ (99%) | |
| 2 | $Co_{0.5}Mn_{0.5}Fe_2O_4$ | $Co(NO_3)_2{\cdot}6H_2O$, $Fe(NO_3)_3{\cdot}9H_2O$, $Mn(NO_3)_2{\cdot}6H_2O$ | 9 |
| 3 | $Co_2Mn_2Sr_{1.66}Nd_{0.4}Fe_{10}O_{22}$ | Co $(NO_3)_2{\cdot}6H_2O$, $MnCl_2{\cdot}3H_2O$, $Sr(NO_3)_2$, $Nd_2O_3$, $Fe(NO_3)_3{\cdot}9H_2O$, CTAB (surfactant), $NH_3$ (as precipitation agent) | 10 |
| 4 | $Ni_{0.25}Co_{0.25}Zn_{0.5}Fe_2O_4$ | NiO, CoO, ZnO, $Fe_2O_3$ | 11 |
| 5 | $Ni_{0.53}Co_{0.12}Zn_{0.35}Fe_2O_4$ | $Ni(NO_3)_2{\cdot}6H_2O$, $Cu(NO_3)_2{\cdot}3H_2O$, $Zn(NO_3)_2{\cdot}6H_2O$, $Fe(NO_3)_2{\cdot}9H_2O$ | 12 |
| 6 | $Ni_{0.48}Co_{0.12}Zn_{0.4}Fe_2O_4$ | $Ni(NO_3)_2{\cdot}6H_2O$, $Cu(NO_3)_2{\cdot}3H_2O$, $Zn(NO_3)_2{\cdot}6H_2O$, $Fe(NO_3)_2{\cdot}9H_2O$ | 13 |
| 7 | $Ni_{0.3}Zn_{0.7}Fe_2O_4$ | $NiCl_2{\cdot}6H_2O$, $ZnCl_2$, $FeCl_3{\cdot}6H_2O$, diethylene glycol, ethylene glycol, polyvinylpyrrolidone (PVP), sodium acetate (NaAc), toluene, 3-(triethoxysilyl)propyl isocyanate (IPTS) | 14 |
| 8 | $Ni_{0.5}Zn_{0.5}Fe_2O_4$ | $ZnSO_4{\cdot}6H_2O$, $NiSO_4{\cdot}7H_2O$, $FeCl_3{\cdot}6H_2O$, $FeSO_4{\cdot}6H_2O$ | 15 |
| 9 | $BaLa_xFe_{12-x}O_{19}$ | $La(NO_3)_3{\cdot}9H_2O$, $Ba(NO_3)_2$, $Fe(NO_3)_3{\cdot}9H_2O$, $FeCl_3{\cdot}6H_2O$, $C_6H_8O_7{\cdot}H_2O$ | 16 |
| 10 | $Ba(LaNd)_xFe_{12-2x}O_{19}$ | $La(NO_3)_3{\cdot}9H_2O$, $Nd(NO_3)_3{\cdot}xH_2O$, $Ba(NO_3)_2$, $Fe(NO_3)_3{\cdot}9H_2O$, sodium dodecyl benzene sulfonate (SDBS), $FeCl_3{\cdot}6H_2O$, $C_6H_8O_7{\cdot}H_2O$ | 17 |

TABLE II. A comparison of properties of hard and soft ferrites.

| Sr. no. | Properties/feature | Hard ferrites | Soft ferrites |
|---|---|---|---|
| 1 | Coercivity | High [exceed 12.5 and go up to 250 A/m]—Oe. Difficult to demagnetize | Low [only a few (A/m)—Oe]. Easy to demagnetize |
| 2 | Examples | 1. $SrFe_{12}O_{19}$ ($SrO{\cdot}6Fe_2O_3$)<br>2. $BaFe_{12}O_{19}$ ($BaO{\cdot}6Fe_2O_3$)<br>3. $CoFe_2O_4$ ($CoO{\cdot}Fe_2O_3$) | 1. $Mn_a\ Zn_{(1-a)}Fe_2O_4$<br>2. $Ni_aZn_{(1-a)}Fe_2O_4$ |
| 3 | Structure of pure ferrite | Hexagonal [vary with impurities] | Cubic [vary with impurities] |
| 4 | Dielectric properties | Dielectric loss decrease with increase of ferrite[a] | Increases |
| 5 | Magneto optical properties | Cause high variation[b] | Cause low variation |
| 6 | Hardness/brittleness | Hard and brittle and close dimensional tolerances can only be achieved by grinding | May not |
| 7 | Categories | Three categories: isotropic, anisotropic and bonded | Not applicable |
| 8 | Uses | Used to make magnets, for devices such as refrigerator magnets, loudspeakers and small electric motors | Used to make ferrite cores for inductors and transformers, and in various microwave components |

[a]Dielectric constant ($\varepsilon'$ and $\varepsilon''$) and dielectric loss (tan $\delta$) are analyzed as a function of frequency and composition and behavior is explained on the basis of Maxwell–Wagner model.

[b]The magneto optical effects or the magneto optical activity is a collective name for a number of phenomena dealing with transformation of the optical wave as it passes through (or reflects from) a magnetic medium. There is, however, essential difference in the origin of magneto optical activity in various parts of the electromagnetic-wave spectrum. Vary in both types; however, variation is more in hard ferrites.

https://doi.org/10.1557/jmr.2017.63 Published online by Cambridge University Press

have been studies showing the effect of cure temperature as a standalone factor on the glass transition temperature of a polymer,[58] the selection of ferrite is not unimportant. A ferrite having $T_C$ well within normal operating temperature ranges should be selected. Usually another term known as "maximum operating temperature" of a ferrite is used which is a safe value of temperature till which a magnetic material should be operated. This is almost 200 °C less than the Curie temperature of magnetic materials and 100 °C above the cure temperature of the matrix. This is adjusted with safety factors taking into account that, no matter what happens, the material becomes a hard magnet while an efficient composite is formed and the matrix does not suffer loss in its properties. A good idea is to select the ferrite in conjunction with the type of polymer. Preferentially, select intrinsic magnetic polymers [thermosets (epoxies)] also known as magneto polymers/magnetic plastics, or ME plastics. These are the polymers which (upon crystallization from melt) as a whole or one phase exhibit response to externally applied electrical or magnetic fields before the addition of external ferrites.[8] They are beneficial as they by themselves are responsive to magnetic field (described in Sec. II). The addition of external ferrites will reinforce this effect. Their use; however is, limited by one or two combinations of inferior mechanical properties which fail the requirements for aerospace structures.

Some other studies based their claim of selection of ferrites on other factors. For example, Jana Rekošová and co-workers[56] showed that magnetic properties such as initial permeability ($\mu_i$) and Curie temperature ($T_C$) are strong function of Ion content ($Ni^{2+}$ and $Zn^{2+}$) for soft NiZn Ferrites embedded in polymeric matrixes [Fig. 3(a)]. An optimized composition $Ni_{0.3}Zn_{0.7}Fe_2O_4$ was proposed for achieving highest value of $\mu_i$ while it was shown that if Zn concentration is increased $T_C$ increase but $\mu_i$ becomes worst. The mechanism behind this magnetic behavior of ferrite samples is attributed to redistribution of ions within

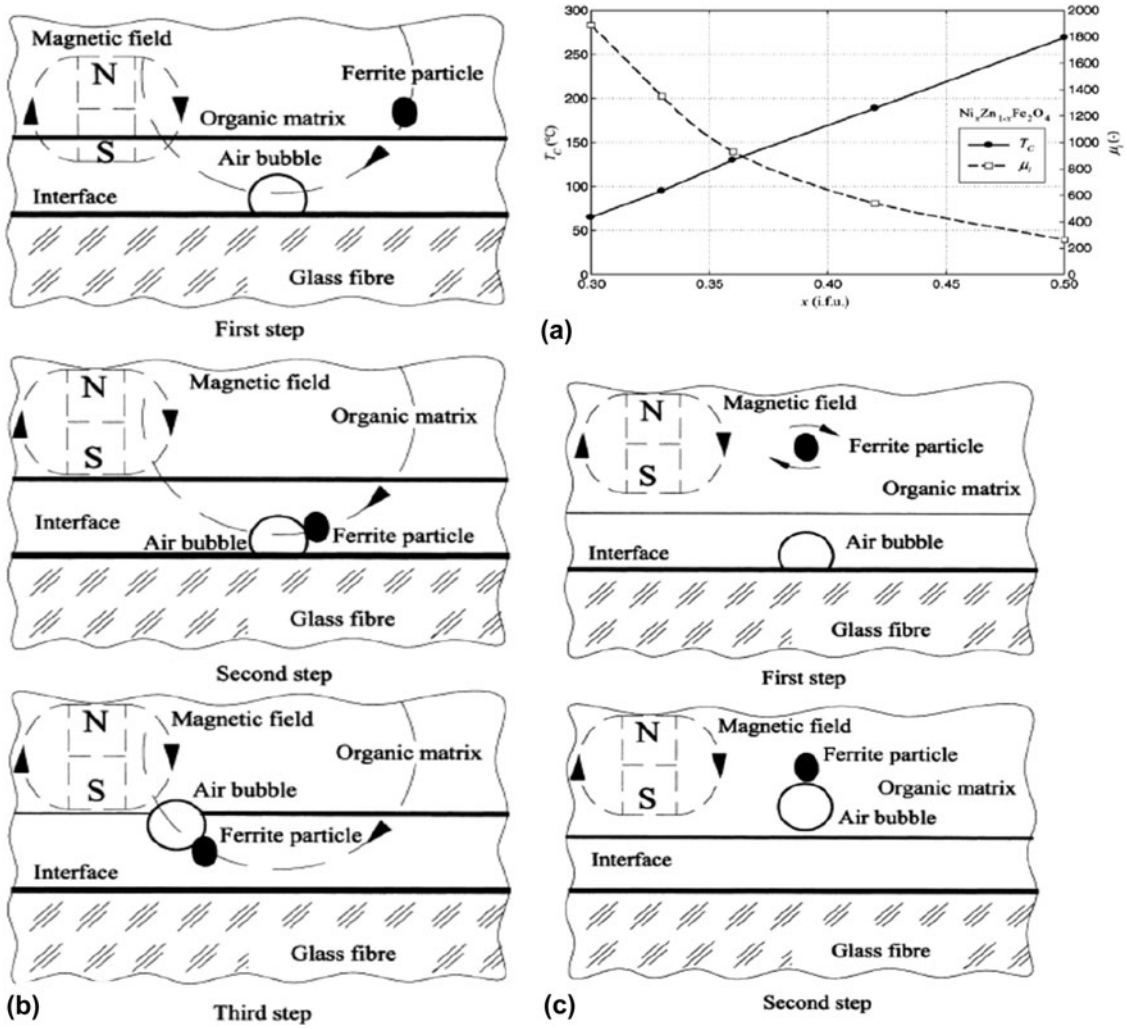



FIG. 3. (a) Dependence of Curie temperature ($T_C$) and initial permeability ($\mu_i$) of $Ni_xZn_{1-x}Fe_2O_4$ for $x$ = 0.30, 0.33, 0.36, 0.42, 0.50,[56] (b) mechanism of bubble formation and dislocation, initial stage (c) final stage.[37]



https://doi.org/10.1557/jmr.2017.63 Published online by Cambridge University Press

tetrahedral and octahedral sub lattices of spinel structure and the variations of the super-exchange interactions in these sub lattices. It was shown that the Curie temperature of the sample ($T_C$ = 65 °C) with the highest value of initial permeability is too low for practical use. Thus, an optimized composition $Ni_{0.33}Zn_{0.67}Fe_2O_4$ was proposed which had $T_C$ = 95 °C at the loss of initial permeability but found to be effective. A similar synergy was observed on the evaluation of mechanical, rheological, and magnetic properties of soft ferrite filled elastomers (natural rubbers).[57]

The details about different polymer matrices that could be used, mechanisms [step reaction (condensation) polymerization, radical chain (addition) polymerization, ionic and coordination chain (addition) polymerization, copolymerization] and processes (extrusion, molding, spinning, vulcanization) involved are described elsewhere[69–75] and are beyond the scope of the present work. Similarly, the details about different mechanisms and processes (hydrothermal, sonochemical, pultrusion, spinning, spin casting, and centrifugal casting) involved for the production of fibers as reinforcements are also described elsewhere[76,78,83–89] and are beyond the scope of the present study. Interested readers can consult standard textbooks, handbooks, and reference articles mentioned for more in depth information about these topics.

### F. Ferrite polymer matrix composites (FPMC)

Numerous studies have been carried out to show the usefulness and effectivity of ferrites (both soft and hard) in polymer matrix composites toward EMI shielding, EMF shielding, self-cleaning, drug delivery, and biomarking, viscosity, magnetic induction, preferential ordering, magnetic confinement, and other directional magnetic properties.

Gabriel Andrei and co-workers[37] used a unique theoretical model to predict the effect of nano ferrite (soft) particles toward removing already formed air bubbles from composite (due to chemosorption) and stopping the formation of further bubbles thus promoting high quality composites. They conducted a series of experiment, employing a range of composites (glass fiber, woven fabric, carbon fiber) and proposed that due to the paramagnetic properties of the oxygen molecule, the air micro bubbles are captured by the magnetic field of the ferrite particles and due to their vibration, it is possible to dislodge and hurl them from the interface to the mass of the polymer matrix, in bonded state. They divided the process into two stages based on time dependent viscosity of composite mixture namely, an initial stage; when the viscosity is smaller than a threshold value $\eta_t$ based on the flow state of the polyester resin [Fig. 3(b)], and a final stage; when the viscosity is higher than $\eta_t$ [Fig. 3(c)]. A detailed description of the mechanisms involved and the parameters affecting these is given in their subsequent works.[38–41] They also studied the effect of different types of dispersion techniques (single step ultra-sonication, and three step magnetic vibration assisted mixing) on the dispersity of filler (5% $Fe_3O_4$) in polymer matrix reinforced with glass fibers. On the basis of a theoretical model, it was assumed that an increase in magnetic particle dispersion will be observed as the system enthalpy increase up to certain optimum value among free enthalpy and system entropy. The results from SEM confirmed that. Also the degree of crystallinity was observed to increase in the latter case due to presence of more nucleation sites at the polymer matrix/fiber interface. This was confirmed as well by the increased value of shear modulus ($G$).[42]

In another study, Stabik, and co-workers[43–45] showed the effect of amount and type of ferrite (hard) fillers on magnetic induction and magnetic properties of epoxy as checked by two different processing routes i.e., gravitational casting (GC) and centrifugal casting (CC). It was found that considerably high values (up to 50 vol% in an increment of 10 from zero) of barium and strontium ferrites can be used as fillers in epoxy. However, detrimental effects toward viscosity increase and further processability were observed for increasing vol% of fillers. It results in air entrapment, coagulation and makes it almost impossible to make pipes via centrifugal casting till 30 vol% and by gravitational casting till 35 vol%. It was also shown that the effect of barium ferrite toward causing an increase of magnetic induction is more than for strontium ferrite and increased magnetic induction is observed in composites with anisotropic fillers rather than the isotropic ones.

They also extended their study to the measurement of viscosity of polymer melts with inclusion of fillers (hard ferrites). They used Hoeppler viscometer with three different temperatures and three different filler contents. The method was only satisfactory for low weight content of solids due to apparatus (degasser) and equipment limitation (size of capillary). Applied method allowed determining the influence of temperature, kind and quantity of filler on viscosity. It was observed that viscosity is inversely proportional to temperature and directly proportional to wt. content of filler. They also showed that viscosity is independent of type of filler. This is attributed to the fact that no chemical reaction occurs between powder and resin. Only physical adsorption happens and is the sole factor responsible for mixing of filler in solution.[46]

### G. Hard magnetic (ceramic) material polymer matrix composites

Dobrzanski and co-workers[47,48] exhibited the effect of mixing of nonmagnetic metal or alloy powders (Fe, Al, CuSn10 and X2CrNiMo17-12-2) in so called magnetic (Nd–Fe–B hardened) epoxies, and studied their processing by innovative one sided uniaxial compaction and

https://doi.org/10.1557/jmr.2017.63 Published online by Cambridge University Press

curing/sintering procedure. They targeted these composites for making magnetic materials for challenging technical application which have space to weight ratio limitations and also require quick processing times (high speed trains, outer and deep space applications). The results found indicated that the presence of nonmagnetic powder particles which interfere with the magnetic particles and result in a decrease in magnetic properties and only the compressive properties increase to an appreciable extent. This is partially attributed to the fact that a range of grain size results in microstructure due to presence of various types of elements with largest for aluminum and smallest for X2CrNiMo17-12-2 high alloy (HA) steel powder. This individually different grain size exhibits different response to applied magnetic field due to unique number of magnetic domains in each grain and thus their overall response vary, resulting in decrease in magnetic properties. Compressive strength increase as voids, porosity, and other manufacturing defects are removed upon compaction and subsequent sintering, resulting in dense, homogeneous, equiaxed grains and in some cases even single phase material. This motivated for further research involving processing of composites with only fine hard magnetic materials without nonmagnetic fillers.

Thus, in a later study,[49] they made composites by the addition of hard magnetic materials (Fe, Nd–Fe–B, and Tb–Dy–Fe) in epoxy based matrices only and studied their processing routes. The results found were encouraging and indicated very high increase in mechanical properties of the resulting composites proving the effectivity of the process. Microstructure also showed complete and well distribution of the hard magnetic nanoparticles in the polymer matrix after curing as well as good compaction, and densification. However, further research is needed to remove bottlenecks (i.e., particle to matrix bonding, inter particle cohesion, decrease in magnetic properties, removal of porosity, anisotropy) in this technology.

Ziebowicz, Szewieczek, and co-workers[50–53] studied the effect of mixing a novel alloy metallic glass $Fe_{73.5}Cu_1Nb_3Si_{13.5}B_9$ with polyethylene of high density (PEHD) in varying percentages. The processing conditions were one sided, uniaxial pressing, and sintering at 170 °C at 200 MPa pressure. The processing involves first attainment of microstructure in strip cast alloy and then mixing it with PEHD. A high temperature (500 °C) sintering practice is adopted for this purpose. This results in α Fe(Si) crystalline and amorphous intergranular phase. The strips were ground to powder in a high energy shaker mill.

### H. Magnetostrictive particles (MSP) polymer matrix composites (PMC's)

Dobrzanski, L.A. and co-workers[54,55] exhibited the effect of addition of magnetostrictive particles (MSP) (Tb–Dy–Fe, Terfenol-D)—particle that undergo expansion/contraction (change in dimensions) under the effect of an applied magnetic field also known as piezomagnetics, in epoxy based matrices and studied their properties. Composite samples of cylindrical shape were made by a casting process and constant stirring was applied to the mold to avoid the sedimentation of particles until compete gelation was achieved. After cross linking was finished, the samples were placed in an oven at 338 K for 5 h to ensure full cure of the resin. Magnetic properties were measured using vibrating sample magnetometer (VSM) and magnetic susceptibility was determined as temperature function on automatic electrobalance. The influence of concentration and particle size of Terfenol-D on magnetic properties were investigated as a function of applied magnetic field intensity, temperature, and frequency. Results indicate that increase in particle size distribution amplifies magnetic response at the same time, growth of resistivity values occurs. Moreover, most importantly, no effect was observed regarding frequency dependence of susceptibility in the investigated frequency range, which indicated and advocated their use in high frequency magnetic field applications.

Kumar and Bhattacharya[59] studied the effect of Terfenol-D MSP layer in between composite layers and used it for real time structural integrity monitoring of composites. They applied MSP layers in between symmetric and asymmetric layers of composites and observed that the MSP layers experience compressive stress while other layers experience tensile stress on the onset of delamination in case of symmetric layers. They also observed that bending stresses are maximum at the surface of layers due to maximum bending (sagging or hogging) there. Also, the effect of MSP detecting damage is more prevalent in case of layers at a distance from center due to maximum bending there. In case of asymmetric layers however, the effect of stacking sequence and orientation of plies play a major role rather than the number of plies itself.

Krishnamurthy and co-workers[60] used the same Terfenol-D MSP layers between multiple layers of CFRP and measured the resulting voltage as a result of delamination occurring on the application of stress. First, they developed nonlinear expressions for co-relating stress–strain, piezomagnetic coefficient, and permeability. Then relations between applied magnetic field in magnetizing coil, magnetic flux density ($B$) in MSP layer, and open circuit voltage induced in sensing coil were developed using previous results. A simulation study was also conducted and a change as large as 68 mV is reported in open circuit voltage on the onset of delamination.

Currie and co-workers[61] used three different layers of Terfenol-D MSP namely 1/8″, ½″, and 1¼″ forming three samples in between layers of CFRP. It was observed and

https://doi.org/10.1557/jmr.2017.63 Published online by Cambridge University Press

shown that voltage decreases with increasing delamination length up to a certain limit beyond which the trend is reversed. The explanation for this was attributed to smaller stress concentrations which yield higher voltage readouts but this trend was reversed by ½″ delamination. It was proposed by them that further experimentation is needed before establishing a defined criterion for such an anomaly.

### I. Magneto rheological elastomers (MRE)

As is evident from name, it is a class of materials which undergo rheology change under the action of applied magnetic field i.e., they become flowable (undergo shear) from viscous condition under the action of an applied field. These are the materials which are classified as magnetic gels in Fig. 1. These can be synthesized and processed by various means ("*in situ*" and "*ex situ*" polymerization) and by incorporation of various types of particles (carbonyl iron) in oils and suspensions to make an intermediate medium which is finally dispersed in an elastomeric matrix [rubbers, polyurethanes (PU), and SEBS].

Anna Boczkowska and co-workers[90] studied the effect of carbonyl–iron particles in a polyurethane matrix. The volume fraction of particles was kept at 11.5%. They used three different types of particles namely carbonyl iron 6–9 μm, carbonyl iron 1–2 μm, and iron powder with an average particle diameter of 70 μm. The elastic modulus $G$ was measured as a function of angular frequency and strength of magnetic field. The highest MRE effect was observed for particles with sizes 6–9 μm and the highest increase in yield stress was observed for samples with particles aligned at 30 °C to magnetic field lines. It was also observed and inferred by them that MRE effect can be varyingly controlled by controlling the microstructure (size, shape, and arrangement) of particles. Stiffness is a strong function of microstructural properties for these materials. A detailed treatment of the subject has been given by excellent authors in the references cited here[91–97] and can be accessed by the interested reader.

## II. THERMODYNAMICS, KINETICS, MECHANISMS, AND PHASE TRANSFORMATIONS

### A. Thermodynamics and formation

Thermodynamic force (Gibbs free energy change) behind the formation of polymer matrix composites and processes involved in their manufacturing strictly helps in explaining the formation of phases, transitions between them, and the evolution of a microstructure. It is the direct answer of the question, whether a reaction/transition will occur or not?

Phenomena like phase formation, thermodynamics, kinetics, transition/transformation, toughening, separation, and microstructure evolution, however, in case of particulates embedded/filled glass fiber reinforced composites (PRC–GFRP) is complex due to presence of multi components which undergo various phase transitions (equilibrium and nonequilibrium) as extrinsic parameters evolve and cannot be explained by one state variable. General physical principles of chemistry and polymer composites do not apply to them. These hybrid composites form two phases mixed together. Their thermodynamic treatment and phase transformation (separation or crystallization) can be explained on the basis of thermally induced changes in "polymer base composite systems" in which polymers are not mixed with other molecules, except at interfaces—the basic definition of composites. These systems typically consist of continuous (matrix) phase and a dispersed (particle) phase. Usually, the matrix phase is formed by polymers. Dispersed particles, in these systems, can have a wide range of shape and size, and play a dominant role in the functional enhancement of the matrix, although never get mixed with the matrix in their thermal/functional history. Interfacial properties are of utmost importance and play an important role in the investigation of these high performance polymer composites. A typical class of these materials is "organic/inorganic hybrid composites" in which the matrix is an inorganic material and the particles are polymeric materials (as explained in Sec. II. E) or vice versa (subject matter of present study).

Any physical mixture of a polymer and ferrites, either pristine or organically modified, does not necessarily lead to the formation of PNCs. For the production of true PNCs, the most important task is to maximize the thermodynamic favorable interactions between polymer matrix and ferrite surface to promote a higher degree of penetration of polymer chains into the three dimensional oxide galleries of the ferrite. This however, is limited by the crystalline nature of the ferrite spinel (straight and inverse) cubic crystals. Furthermore, mostly under microscope, these ferrite crystals are exhibited as platelets having a distinct size a few microns wide and a few hundreds of nm thick. Typically, it is rare to get hexaferrite platelets below about 300 nm diameter.[7] If ferrite platelets ultimately phase separate from the polymer matrix, the composite will not exhibit the expected improved properties. Therefore, it is also essential to understand the macroscopic phase behavior of the final composite. The main aim of this section is to summarize the thermodynamics, kinetics, and molecular modeling of PNC formation. Like immiscible polymer blend systems, the thermodynamic mixing of polymer chains and ferrite particles can be described through a balance of entropic and enthalpic factors, which determine the nanoscale dispersion of ferrite particles in a polymer nanocomposite (PNC). In case of the ferrite particles, favorable thermodynamics of mixing are essential because ferrite platelets (one

https://doi.org/10.1557/jmr.2017.63 Published online by Cambridge University Press

complete or a set of unit cells) by nature are held together by very high attractive forces. Therefore, purely extensive mechanical methods (such as strong mechanical mixing, extrusion, melt, and mixing) of dispersing ferrite particles into a polymer matrix are not effective.[98]

Since no formal treatment of this problem and no data exists in the literature till date, the authors will present a theory of their own to explain the phenomena of composite formation in case of ferrites embedded in fiber reinforced composites (FRP) (also known as hybrid FRC–MPMC). This can be explained by two means (i) the Kelvin equation—which describes the interaction and dissolution of a crystal in a liquid melt (prevention of Ostwald ripening) and (ii) by the "layer moiety theory" in which ferrite platelets are treated as distinct layers. This theory is based on the general interaction of layered materials [i.e., clay like, silicate like, oxides, hydroxides,[98] layered hydroxy salts (LHS)[99]] with under laying organic layer and is assumed to be applicable for all types of layered/platelet structures (such as ferrite platelets).

It will be explained step by step. First the use of the Kelvin equation dictates that the "characteristic length" is to be determined and it should further dictate the avoidance of Ostwald ripening. The only way a filler particle's inner phase couples with environment (surrounding) of particle, is through its interface. The particle's solubility couples through particles' radius of curvature, following Lord Kelvin equation. This also explains Ostwald ripening (i.e., a difference in solubility between large and small particles in terms of a difference of chemical potential). Smaller particles have a higher solubility than larger ones

$$S(r) = S(\infty)\exp\left(\frac{2\sigma V_{\mathrm{m}}}{rRT}\right) \quad . \tag{1}$$

where $S(r)$ is the solubility of particle having radius $r$, $S(\infty)$ is solubility of filler with infinite radius of curvature, $\sigma$ is Gibbs interfacial energy between particle surface and polymer matrix. $V$ is the molar volume of dispersed (filler) phase, $R$ is the gas constant, and $T$ is absolute temperature. $S(\infty)$ can be determined experimentally and $S(r)$ will not become noticeable until $r$ is very small. The quantity $\left(\frac{2\sigma V_{\mathrm{m}}}{rRT}\right)$ is called characteristic length. It has an order of ~1 nm or less, indicating that difference in solubility of a 1 μm particle is of the order of 0.1% or less. Theoretically, Ostwald ripening should lead to condensation of all particles into single. This, however, does not occur in practice (which is an advantage) since rate of growth decrease with increase of particle size. Factors affecting rate of Ostwald ripening are surface phenomena (surfactant micelle), impurities and nature, type and amount of surfactant themselves (block or graft polymers).

Secondly, for better explanation in terms of "layer moiety theory", consider an interfacial formalization[100,101] between two flat layers (such as ferrites) separated by an organic layer (such as alkyl surfactant or intercalated polymer). According to analysis, the successive layers are held together by an adhesive energy

$$\Delta F_{\mathrm{sas}} = -2\gamma_{\mathrm{sa}} = -2\left(\sqrt{\gamma_{\mathrm{s}}^{\mathrm{LW}}} - \sqrt{\gamma_{\mathrm{a}}^{\mathrm{LW}}}\right)^2 - 4\left(\sqrt{\gamma_{\mathrm{s}}^{+}} - \sqrt{\gamma_{\mathrm{a}}^{+}}\right)\left(\sqrt{\gamma_{\mathrm{s}}^{-}} - \sqrt{\gamma_{\mathrm{a}}^{-}}\right) \quad . \tag{2}$$

Consider the layer additivity of apolar [such as Lifschitz-van der Waalz (LW)] and polar [such as electron donor acceptor or Lewis acid–base (AB)] interaction terms, then below can be written following standard geometric combination rules

$$\gamma_{ij} = \gamma_{ij}^{\mathrm{LW}} + \gamma_{ij}^{\mathrm{AB}} \quad , \tag{3}$$

where

$$\gamma_{ij}^{\mathrm{LW}} \cong \left(\sqrt{\gamma_i^{\mathrm{LW}}} - \sqrt{\gamma_j^{\mathrm{LW}}}\right)^2 \tag{4}$$

$$\gamma_{ij}^{\mathrm{AB}} \cong 2\left(\sqrt{\gamma_i^{+}} - \sqrt{\gamma_j^{+}}\right)\left(\sqrt{\gamma_i^{-}} - \sqrt{\gamma_j^{-}}\right) \quad . \tag{5}$$

The $i$ and $j$ subscripts corresponds to the various system components (ferrite, f, alkyl surfactant layer, s and polymer, p) and LW and AB superscripts are related to the nature of the interactions, that is, apolar LW and polar AB.

These relations can be converted into the Hamaker constant formalization by putting

$$\gamma_{ij}^{\mathrm{LW}} = \frac{A}{24\pi I_0^2} \quad . \tag{6}$$

Where $I_0 = 1.58$ Å.

Like other similar composite systems, under suitable conditions, for ferrite polymer matrix composite (FPMC), interaction energy shown above [Eq. (1)] can be converted to adhesive pressure ($P$) between parallel surfaces.

$$P = \frac{A}{6\pi d^3} = \frac{-12\pi I_0^2 \Delta F_{\mathrm{sas}}}{6\pi d^3} \quad . \tag{7}$$

where $d$ is thickness of organic interlayer film.

This relationship between energy (expressed as adhesive pressure) and interlayer thickness for a generalized ceramic material (bi layer) separated by organic layer can be described by following figure [Fig. 4(a)].

https://doi.org/10.1557/jmr.2017.63 Published online by Cambridge University Press

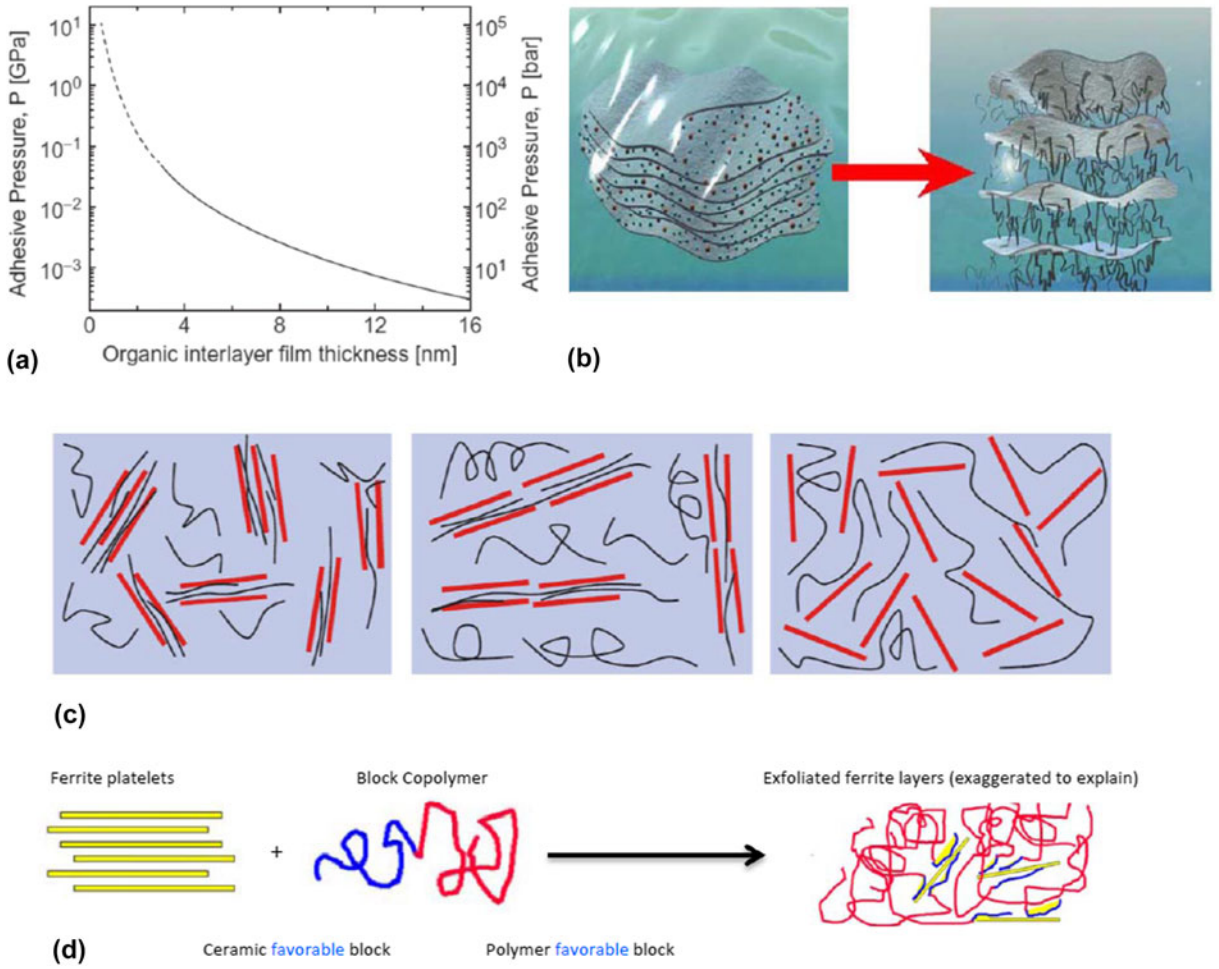



FIG. 4. (a) Adhesive pressure versus interlayer thickness for two flat ceramic surfaces separated by apolar organic film (such as olefin)[101] (b) schematic of ion exchange reaction. The inorganic ions (small in size) are exchanged against huge organic onium cations. This type of reaction has two consequences (i) gaps between sheets (platelet) are widened, enabling polymer chains to move in between them and (ii) surface properties of each sheet (platelet) are being changed from hydrophilic to hydrophobic.[145] (c) Three types of thermodynamically achievable PNCs having polymer as matrix and ceramic fillers as reinforcements (left to right: intercalated, exfoliated and flocculated).[104] (d) Schematic of action of bock copolymer for an exfoliation of ferrite platelets within a polymeric matrix (drawn out of scale).

It can be seen easily that this relationship is nearly inverse, which means as the pressure (energy) between layers increases; a smaller interlayer thickness is sufficient to maintain equilibrium/promote formation. This explains that favorable enthalpic interactions between a "ferrite surface–interlayer–polymer matrix" are necessary for ferrite particle dispersion at the nanoscale and for nanocomposite formation. It has been suggested by numerous studies on clay by Vaia et al.[102,103] that small per-monomer favorable enthalpic interactions can derive dispersion of these nanofillers in the polymer, and promote the formation of a composite. These favorable enthalpic interactions are an excess enthalpy and from Florey–Huggins theory: for a ceramic filler (i.e., ferrite) modified by surfactant and polymer, favorable enthalpy of mixing is achieved when the "polymer matrix/inorganic filler (ferrite) interactions" are more favorable than "surfactant/inorganic filler (ferrite) interactions". Thus, the polymer base will tend to promote the formation of a composite by allowing dissolution of ferrite in it. It is also known that, dispersion would dictate a negative interaction energy change (upon mixing), which corresponds to a positive interfacial tension difference. Thus, for most polymers, the commonly used organic modification by alkyl—cationic surfactant is adequate to create sufficient excess enthalpy and promote nanocomposite formation with layered ceramics. In a different way, a "larger macromolecule surfactant" that would increase the layer separation to 5–10 nm makes provision for much smaller enthalpic contribution since due to inherent nature of parting apart the layer; it eliminates the need to overcome huge adhesion (which is about thousand times smaller). An example of such mechanism is polypropylene.[104] However, no practical evidence exists in

https://doi.org/10.1557/jmr.2017.63 Published online by Cambridge University Press

literature of exfoliating ferrite layers and treating them as separate layers for incorporation of polymer chains in them which eventually will lead to formation of PNCs. A crystallographic study may help resolve the situation if such a moiety is formed or not.

### B. Interaction of polymer systems—formation of nanocomposites (PNCs)

Typically, for the layer moiety theory, based on how the polymer chains and ceramic nanoparticle interact, there are three types of PNCs [Fig. 4(c)]. (i) *Intercalated PNCs*: in intercalated PNCs, the insertion of polymer chains into the ceramic (ferrite) layered (platelet) structure occur in a crystallographically regular fashion, regardless of ferrite–polymer ratio. Intercalated PNCs normally feature interlayers composed of a few molecular layers of polymer. The properties of such composites typically resemble those of ceramic materials. (ii) *Exfoliated PNCs*: in these types of composites, the individual ceramic layers (platelet) are separated in a continuous polymer matrix by an average distance that depends on ceramic filler loading. Usually the filler content of exfoliated composite is much lower than that of intercalated PNCs and (iii) *Flocculated PNCs*: they are the same as intercalated PNCs. The difference being is that the oxide layers (platelets) of ferrites are sometimes flocculated due to hydroxylated edge–edge interactions of platelets.

### C. Mechanism of inter-layer action

In this subsection, we will explain how inter-layer between polymer and ceramic (platelet) act to create a medium through which interaction of both becomes possible and sustainable. Different materials have been tried and tested over time to be used as fillers and with the change of chemistry and structure of each, the requirements of the interlayer also changed. However, the smaller the reinforcing composite elements are, the larger is their internal surface and hence their tendency to agglomerate is increased, rather than to disperse homogeneously in matrix. A successful approach to disperse these nanoparticles in a matrix involves the swelling of layers (in case of perfect layered materials) via an exchange process of the cations located between the crystalline layers against organic onium type cations [Fig. 4(b)]. The approach is very successful and currently enforced in practice with clays as described in previous reports.[102,103] These cations are required to have another functional group to react with monomers, oligomers, or polymers in a subsequent step to separate the platelets completely from each other and/or to finally form matrix material with homogeneously dispersion platelets (molecular composites).[105–108]

In these cases, the growing chains are grafted (closely attached) onto the nanoparticles and act as compatibiliser (a material which acts as bridge between organic polymer and ceramic filler platelet) and matrix material at the same time. However, the shortfall of this technique is that it cannot be applied to all material combinations, since the synthesis of some materials, e.g., polyolefines, is by far more complex than the synthesis of polyamides. In a similar way, although theoretically proven to be very promising, attempts to incorporate nanoparticles in a polymer matrix simply by a surface modification of the particles using the ionic interaction with surfactant molecules gained only a moderate success or failed completely. In most of the cases, the natural agglomeration tendency of the nanoparticles has either been difficult to overcome or led to thermodynamically instable mixtures. A practical solution of this problem is to consider three components of the system namely (i) particle (surface), (ii) interfacial component (surfactant) and (iii) matrix polymer chains. This is done to ascertain that interaction enthalpy between surfactant molecules and the polymer chain may be the deciding value for a thermodynamically stable, homogeneous incorporation of nanoparticles into a matrix material. Vaia et al.,[102] developed a mean field based theory to understand and explain the impact of different interaction enthalpies onto the possibility of dispersion of particles in a polymer matrix. They explained three different interactions, namely polymer–surfactant interaction, surfactant–surface interaction, and polymer–surface interaction. The calculations lead to very important conclusions in polymer filler mixing theory. They inferred

(i) Even when surfactant chains are miscible with the matrix polymer, a complete separation depends on establishment of very favorable polymer–surface interactions to overcome penalty of polymer confinement.

(ii) If this is not the case, a good dispersion of particles may be reached by the help of strong shear forces during preparation and processing of PNC. However, the system will remain thermodynamically unstable. If such a mixture is heated to a temperature above the melting point, immediately a partial re-agglomeration of particles took place (evolution of metastable state) (Ostwald ripening).

Another proposed method is to decrease the strength of interactions surfactant–surface and surfactant–polymer interfaces which lead to interaction strength polymer–surface (much desirable), for example by the use of fluorinated surfactants. Dramatically high values of elastic moduli (up to 60%) and strength (up to 40%) along with a decrease of permeability (up to 10%) for gases such as Ar, $O_2$, and water vapor have been achieved with proper exfoliation of only small amount (5%) of filler as loading.

### D. General process of nanocomposite (NC) formation

Formation or processing of nanocomposites (NCs) largely depends on how both parts (ceramic and polymer)

https://doi.org/10.1557/jmr.2017.63 Published online by Cambridge University Press

which are intrinsically immiscible interact to form a thermodynamically and kinetically stable composite.[79–82] This process is greatly facilitated by the use of compatabilising agents. An ideal compatibilisation agent between two intrinsically noncompatible components (ceramic and polymer) should have parts (combined in one molecule) which should physically mix easily in a thermodynamically stable manner with both components. Surfactants fulfill only partly this requirement, the ionic part interacts certainly in a favorable way with the charged surface of the ferrite platelets. However, long alkyl tail (for example), displays only a limited compatibility with the polymer chains. Secondly, as stated before, polymer–surface interactions are important for a complete and stable dispersion as well. A better compatibilisation should be expected from "macro-surfactants" like block or graft copolymers combining blocks which have the property of interacting with the solid particle surface (ceramic nanoferrites) and with the matrix polymer and thus meeting the most of the requirements listed above. This interaction is schematically shown in Fig. 4(d). In some cases, block copolymer can also be used as "co-surfactant" next to surfactant on the surface of ferrite platelets thus fine tuning the thermodynamic characteristics of the ferrite with respect to the polymer matrix material. In general, ferrite polymer matrix nanocomposites can be formed by any of "top down" or "bottom up" approaches as is routine practice in nanotechnology. In "top down" approach, the starting point is bulk material and it proceeds by mechanical attrition. The process is energy extensive and generates a range of particle size and thus quite limited for practical use. In the "bottom up" approach on the other hand, the starting materials for the synthesis of PNCs are monomers and molecular precursor of magnetic component. The basic processes involved in these approaches are (i) polymerization of monomer (ii) formation (precipitation) of magnetic component and (iii) mixing of magnetic and polymer component.

These steps can be reached by any of following combinations

(i) Separate polymerization and precipitation.

(ii) Simultaneous precipitation and polymerization followed by mixing.

(iii) Precipitation and mixing followed by *in situ* polymerization.

(iv) Polymerization and mixing followed by *in situ* precipitation.

**(i) Separate mixing of polymer and magnetic component ("*ex situ*" method)**: This process can be used to form films and bulky materials. This can be achieved by dispersing the magnetic component in a polymer solution or a polymer melt and then making the film by evaporating, spin casting or cooling. This can also yield core–shell structures. The binding of polymer to particle surface is achieved in a similar way as described in Sec. III for ceramic layers (i.e., binding by electrostatic charge). The stability of nanocomposites suspension can be reinforced by crosslinking of the polymer after coating (in case of coated products). Another process described, makes use of bi functional layers. Yet another process advocates for simple method of formation of coated particles by non-solvent assisted precipitation followed by fast cooling. **(ii) Simultaneous precipitation and polymerization.** This can be performed by co-condensation of the monomer and precursor vapors. The main advantages of this method are high homogeneity and a strong polymer–particle binding. This is a very popular method for the production of metal–polymer nanocomposites (such as those with polyamides, polyimides, polystyrene, and teflon). A variant of it make use of UV irradiation and yield further superior properties with respect to particle size and its distribution.[109] **(iii) "*In situ*" polymerization**: This type of polymerization can be carried out in case of dispersion of particles in a monomer solution or in a monomer melt. This route is especially suitable for the preparation of nanocomposites with a high density of particles when the polymer is insoluble or it does not melt. For further enhancement of cohesion, particles can be grafted to the polymer surface by irradiation or homogeneity can be increased by sonochemical polymerization. This yields excellent core–shell structures with a tunable shell thickness. This is an excellent route to achieve strong particle–polymer binding by preactivation of the particle surface with a reactive residue, polymerization initiators or own monomer. Examples of such reactions are polyimide–bonded magnets of rare earth alloys. **(iv) "*In situ*" precipitation**: This is another excellent method for processing of films and bulky materials. It facilitates a controlled particle growth, a regular particle-polymer interphase, a uniform distribution of particles in the matrix, and even microstructural organization (Fig. 5).

Polymer and metal precursor can be mixed by

(i) Absorption of metal ions in ionic exchange resins or in polymer gels.

(ii) Dissolution of the precursor in a polymer melt, or a polymer solution.

(iii) Deposition of the precursor in a porous polymer by chemical, electro-chemical, or physical (vapor) methods.

Then particle growth is achieved by standard growth [nucleation and growth (NG)] mechanisms. The size and the shape of the particles can be controlled with the precursor/polymer ratio, the molecular weight of the polymer, and the relative chain length in block copolymers. Examples of this process are iron oxide NCs, metal (Cr, Mo, W, Fe, Co)—NCs, Co NCs, FePt NCs, NiFe nanowires, magnetic tapes by deposition of metal vapors on polymer substrates.

https://doi.org/10.1557/jmr.2017.63 Published online by Cambridge University Press

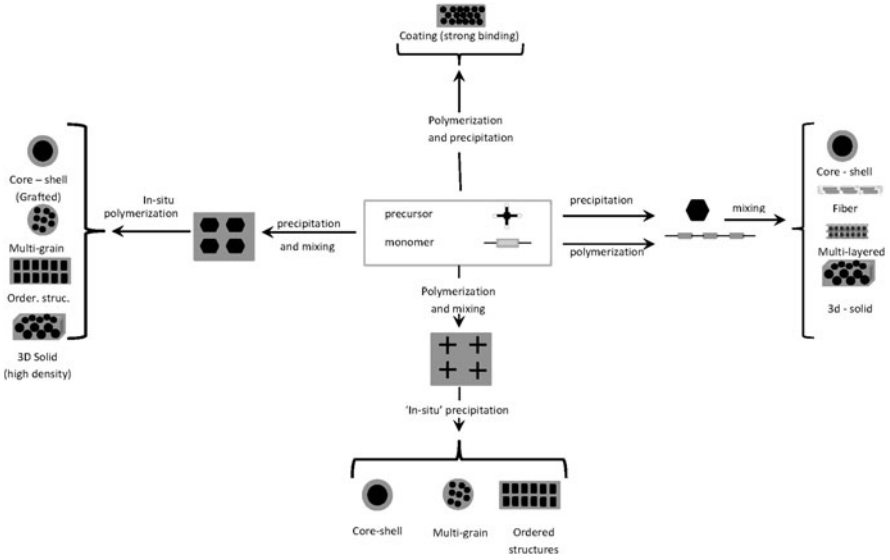



FIG. 5. Different synthesis routes for preparation of magnetic polymer composites.[109]

## E. Nanostructure formation

After all moieties, nanostructures can be formed by the polymer (matrix confinement, programmed assembly by molecular recognition), the inorganic component (inter particle conjunction, shape directed assembly), the substrate (substrate engineering), or a magnetic field. Laminar stacking in hybrid (organic–inorganic) composites can be achieved via a variety of methodologies. For example, Langmuir–Blodgett films, sequential deposition of polyelectrolytes, layer by layer (LBL) assembly and two-dimensional perovskites. However, the most versatile route for the fabrication of ordered magnetic nanostructures is based on the use of block copolymers (as discussed above). Diblock-copolymers of linear $(A)_n(B)_m$ chains form self-assembled structures in the solid state that can be maintained in a length scale of centimeters. The shape of the structures can be changed with the values on n and m from spheres to cylinders, gyroids, and lamellae which are a very powerful tool to control the microstructure and resulting properties. Furthermore, the selective dissolution of one of the blocks followed by crosslinking and selective degradation lead to a large variety of nanostructures: i.e., hairy nanospheres, shaved nanospheres, porous nanospheres, hollow nanospheres, nanospheres with cross linked shells, cross linked polymer brushes, nanofibers, and nanochannels in polymer thin films. Some of key block copolymers proposed for the fabrication of ordered magnetic nanocomposites are: aniline and formaldehyde, poly(norbornene-dicarboxylic acid) and poly (norbornene), poly(4-vinylpyridine) and vinylstyrene-4-vinylpyridine, poly(styrene-*b*-2-vinyl pyridine), acrylonitrile-methyl methacrylate-divinyl-benzene and polystyrene-polymethylmethacrylate. A new trend in developing nanostructures is to make use of nature's own power and ability to synthesize nanostructures. Living organisms such as magnetotactic bacteria and viruses have been genetically manipulated and controlled to produce a variety of magnetic nanostructures (Fig. 5).[109]

## F. Characterization

Magnetic nanocomposites are composed of magnetic particles, wires or layers (platelets) which are embedded in a polymer matrix. Thus, the specific characterization for magnetic nanocomposites must focus on the determination of particle size and shape, coating thickness; inter particle distance, and particle–polymer interphases, and magnetic structure, in the nanometer scale. To this end, scanning probe microscopies and electron microscopy give direct information about nanostructures but they are confined to a small area of the material. On the other hand, radiation scattering methods are indirect but non-invasive, sample preparation is easy, and they give useful information about particle size, coating layer thickness, and particle ordering. Moreover, electron energy loss spectroscopy (EELS) yields local chemical information (interphases), and holography and neutron scattering give information about local magnetic structures. Here only a short description of each method will be presented as a detailed treatment of the subject requires a review of its own and is beyond the scope of the present work. Although primitive, Optical microscopy is the best technique used to study phase transitions (as these are light contrast sensitive) and optical microscopy can yield direct, clear, and precise information about phases present in an inexpensive way. The disadvantage include that it does not provide information on nanoscale due to limitation of wave length of light. Problems encountered

https://doi.org/10.1557/jmr.2017.63 Published online by Cambridge University Press

at nanoscale can best be addressed via electron microscopy. Transmission Electron Microscopy (TEM) at its one end, being powerful to yield information about phases, transformation products, inter-particle structure and morphology at nanometer scale, also possesses the ability to yield information about the chemical structure of materials on the other end. This is because various types of auxiliary energy signals are produced during investigation and interaction of electron with matter which can be read using proper detectors and used toward knowing in detail the chemical makeup of a material. High resolution electron microscopy (HREM) is a variant of electron microscopy which provides information about the structure of a material at atomic lattice scale. The lattice fringes seen in HREM images are closely related to atomic phases in specimen. Intereticular distances as well as angles between crystallographic planes can be easily measured by HREM. This technique, however, has a limitation of not being able to measure nonperiodic nanostructures. Further, this technique is very sensitive to minute geometrical changes in the environment surrounding specimen. HREM simulations are needed to accurately predict structures without errors. Another way of achieving this is to combine HREM with averaging techniques such as WAXS or EXAFS. An example of use and affectivity of these techniques is determination and identification between magnetite ($Fe_3O_4$) and hematite/maghemite ($Fe_2O_3$). They both are completely indistinguishable in ordinary HREM but their EELS spectra and radial distribution factor (RDF) is completely different. Similarly wide angle X-ray scattering (WAXS), small angle neutron scattering are also used to observe and note phases formed, their type, abundance, and distribution. Compared to TEM they have advantage of easy sample preparation, rapid measurement, and large areas of resolution and possibility of "*in situ*" observation.

### G. Kinetics and phase transformations

Primarily, in polymer melts reinforced with particles, crystallization or phase separation can occur by any of "liquid–solid" or "solid–solid" transformation mechanisms. Former case is dominated when thermoplastics are present as matrix. The resulting phase could be single or poly-crystal, fully crystalline or semi-crystalline (SC) polymer and morphology would be facets, platelets, globules, spherullites, cracks, and crazes. There are countably a few exceptions to this when the structure formed is amorphous [PMMA, polycarbonate (PC)] but the predominant phenomena is as described before. A detailed treatment of this subject can be found in standard texts and articles on phase transformation in polymers.[110,111] Furthermore, void formation due to release of oxygen and volume shrinkage occurs in case of these matrixes. Most of the phenomena in these polymers are governed by complex laws of rheology and computational fluid dynamics (CFD). A phase diagram (just like in case of metals and alloys) is needed for explanation of appearance of phases, critical transformation lines, lever rule (tie lines) etc. In later case [present situation—thermosets (epoxies)], however, toughening primarily is achieved by the curing process. An explanation of how this happens can be given by curing kinetics which is briefly described here. Curing reactions involves various phenomena during their occurrence which are a multitude of their composition and constituents. For example, during curing, large molecules with higher molecular weights are formed by cross linking bonds. As a result of this, as the reaction progresses, the available volume in the molecular arrangement decreases, resulting in (i) shrinkage and (ii) less mobility of species, thereby affecting the viscosity of the resin. This results in diffusional factors dominating and taking the lead in controlling the process rather than chemical factors. There are two types of cure reaction of thermosets. (i) Step (epoxies, phenolics and urethanes) and (ii) chain (unsaturated polyesters, vinyl esters, acrylates) polymerization. In first, the size of the chain increases because of linking of oligomers to themselves while in second case, the size increases as a result of the addition of monomers at the end of chain. In both cases, however, thermosetting resins cure chemically to form a crosslinked network, becoming rigid, solid, chemically inert (insoluble), and thermally stable.

A curing reaction can be characterized in several ways.

(i) Kinetic models: relating reaction rate to temperature, and degree or extent of cure.

(ii) Gelation theory: relating $T_g$ to degree of cure.

(iii) Rheological models: relating resin viscosity to temperature and weight average molecular weight.

For practical purposes and applied situations, they are all connected to each other.

**(i) Kinetic models**: The mechanism of curing of thermosetting resins is very complex because of relative interaction between chemical kinetics and the changing of physical properties and is not yet fully understood. There are two distinct approaches how this problem is addressed (i) *phenomenological* (macroscopic level) approach and (ii) *mechanistic* (microscopic level) approach. In simplest form, former is related to an overall reaction (i.e., when only one reaction represents the whole process) and later is related to kinetic mechanism for elementary reactions occurring during the whole process (step by step study). The phenomenological models are semiempirical and hence do not provide a clear description of the curing process and its chemistry which is important for understanding the network formation process. The *mechanistic* models, however, are more representative of the resin curing kinetics because they

https://doi.org/10.1557/jmr.2017.63 Published online by Cambridge University Press

are based on stoichiometric balances of reactants involved in the elementary reactions. Thus, they are much more complex than the phenomenological models, but they are a true representation of the kinetics of cure. The physical and mechanical behaviors of the cured resins are determined by the chemical reactions that occur during curing. The understanding of the mechanism and kinetics of cure is one of the most important steps in evaluating the structure–property relationship of thermosets. Thus it is helpful to know all the possible reactions for a particular system and control the processing conditions to tailor the results according to your yield. The reactions occurring during curing are so complex and so many that even a mechanistic approach cannot solve all the problems. An effort to achieve simplicity by making the problem more complex is not a justifiable approach. Thus, due to lack of rigor, phenomenological models are more widely adopted and used to solve curing kinetics problem. **(ii) Gelation theory**: Curing (cross linking chemical reaction) cause changes in physical properties of the substances involved such that an increase in molecular weight and resin viscosity results. There are two critical points about these changes. *Gelation* and *vitrification*. *Gelation* is responsible for the transformation of resin from liquid to rubbery state whereas *vitrification* takes place when glass transition temperature ($T_g$) increases to and equals temperature of cure, making transformation from a rubber to a gelled glass (onset of gelation) or from liquid to ungelled glass (no onset of gelation). These transformations can be explained well by a standard diagram known as time temperature transformation (TTT) diagram which explains nonequilibrium cooling and formation of nonequilibrium phases (Fig. 6). This is very similar to the TTT diagram in metallic alloys which form the basis of nonequilibrium heat treatment (martensitic transformation) of the majority of steels.

It can be observed that five states may exist namely ungelled glass, liquid, gelled glass, gelled rubber, and

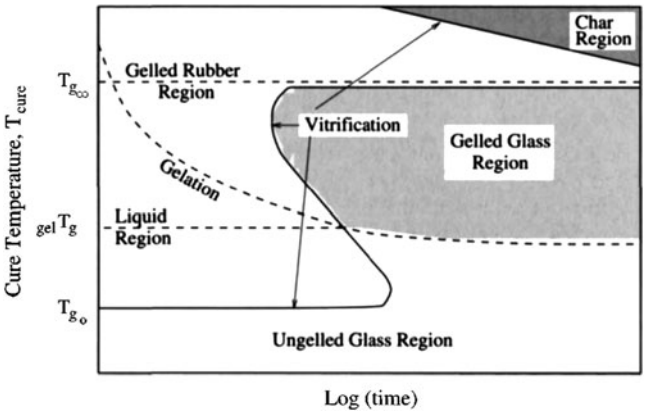



FIG. 6. Time–temperature–transformation (TTT) cure diagram of polymer system.[115]

char. The S-shape curve (gelation and vitrification) delimits the resin state and three critical temperature result. The glass transition temperature of reactants ($T_{go}$), gelation and vitrification simultaneous occurrence temperature ($_{gel}T_g$), and glass transition temperature of fully cured system ($T_{g\infty}$). No reaction occurs below $T_{go}$ as reactive species are seized for motion in the glassy state. Kinetics of reaction above $_{gel}T_g$ has only been explained partially to increase, decrease, or stay constant for few systems.[112–114] As a rule of thumb, a fully cured resin is only achieved when cure temperature is higher than ($T_{g\infty}$) (as described in Sec. II. C) (with no vitrification thus allowing for the moment of molecules, and as a result, reaction). Also, cure temperature can neither be too high nor can it stay at higher temperature for long periods of time as it will result in (thermal) degradation (charring) of the resin (not desirable). This theory has been explained in various models to explain the onset of gelation by statistical, probabilistic, and deterministic approaches. **(iii) Rheological models**: The viscosity of the resin during curing is a function of time, temperature and degree of cure. For non-Newtonian resin melts it is a function of shear rate as well. Two concurrent phenomena are responsible for explaining and determining the rheological behavior of composite systems. (i) *Intensification of mobility*: decrease in viscosity because of increase in temperature (ii) *increase in viscosity due to growing size of molecules during cure*. Free volume theory (intrinsically conditional movement of molecules in the amount of free volume in a molecular ensemble which explains slow response to a perturbation in equilibrium state in terms of more collisions among molecules being inversely proportional to less unoccupied space) is well used to explain this in the form of empirical relationships.

The first phenomena is well explained by the William–Landel–Ferry (WLF) equation

$$\ln\frac{\eta}{\eta T_0} = \frac{-C_1(T-T_0)}{C_2+T-T_0} \quad . \tag{8}$$

where $C_1$ and $C_2$ are adjustable variables and $T_0$ is reference temperature.

While the second phenomena is explained by the Enns and Gillham equation

$$\ln\eta = \ln\eta_\infty + \ln\overline{M}_w\frac{E_\eta}{RT_0} = -\frac{C_1(T-T_0)}{C_2+T-T_0} \quad , \tag{9}$$

where $\eta_\infty$ = extrapolated viscosity and $T \to \infty$, $E_\eta$ = activation energy, and $\overline{M}_w$ is weight average molecular weight.

Here $T_0$ = arbitrary chosen reference temperature above which Arrhenius equation is valid to describe viscosity–temperature dependence.



https://doi.org/10.1557/jmr.2017.63 Published online by Cambridge University Press

The "last stage" of curing is characterized by "diffusion equations".[115] This is because during the last stages, chain growth, and crosslinking of atoms occur as a result of which movement of reactants slow down or cease near gel point resulting in increase of viscosity. Thus the curing process is controlled by these diffusional motions rather than by chemical factors. As a consequence, special techniques such as dielectric permittivity, dielectric loss factor, ionic conductivity, and dipole relaxation time are used because spectroscopic techniques are ineffective because of insolubility of reaction mixtures at high conversions. In empirical terms, behavior during this stage is described by addition of several factors in phenomenological equations.[116] Generally speaking, curing and subsequent transformations in thermosets are solid–solid transformations. These are strictly temperature dependent transformations carried out in a solidified and cured crystalline/semi crystalline (SC) mass. They involve no melting or softening. These are very similar to heat treatment in metals and alloys (as described earlier). They can either occur by nucleation and growth (NG) or spinodal decomposition (SD). Each has its own mechanisms and is triggered only in certain situations. Separation occurs in the form of primary and secondary transformations. Interconnected phase is formed as a result of spinodal decomposition (primary phase separation) while regularly repeating periodic phase coalesce to form droplet–matrix (sea–island) [nucleation and growth (NG)] type morphology (secondary phase separation). This secondary phase separation occurs in both droplets as well as in matrix phase. For example, for polyetherimide (PEI) modified diglycidyl ether of bisphenol A (DGEBA) and PEI modified bisphenol A dicyanate (BPACY). Usually at lower filler content ($<$10 wt%), transformation proceeds via nucleation and growth (NG) mechanism exhibiting sea–island morphology while for higher concentrations ($>$25 wt%) phase separation occurs by spinodal decomposition (SD) mechanism and nodular morphology was observed. At intermediate compositions, dual phase morphology with both sea–island and nodular morphology was observed (Fig. 7).[117]

Properties of a thermoset polymer such as $T_g$, phase separation and ordering are explained on the basis of these separations. A detailed explanation of these properties is given in the next section. Various factors such as surface energy, molecular weight, shape and size of particulate reinforcements, diffusion, surface phenomena, energy transfer and conformational changes all contribute toward formation and evolution of the microstructure in these transitions.

## III. PROPERTIES

Various studies have been carried out to determine and measure properties of both thermoplastic and thermosetting filled polymer systems. A huge emphasis is laid upon measurement, determination, and optimization of mechanical properties over the years, especially for thermosetting systems. It is only very recently with the advent of microelectronics, photonics, optoelectronics, and nanotechnologies that research trends have expanded into the measurement of thermal, electrical, optical, and in our case magnetic properties. A tale of each is briefly described below, along with nondestructive evaluation.

### A. Density or specific gravity

Used synonymously, density or specific gravity may be defined as mass per unit volume in case of "density" and weight of a substance in relation to the weight of an equivalent amount of water in case of "specific gravity". Density is determined by the size of atoms forming the mineral, abundance with which they are packed together and the amount, type, nature, and abundance of impurities hindering the packing of atoms. The closer the atoms are packed together, the higher will be the density. Thus, smithsonite ($ZnCO_3$) has a much higher specific gravity as compared to calcite because the mass of Zn is much higher than the mass of calcium. Conversely, magnesium has higher specific gravity than calcite despite the fact magnesium is lighter than calcium. This happens as ions of magnesium pack much closely together than calcium thus contributes toward increase of specific gravity. True specific gravities of particulate additives can range from less than 1.0 for hollow glass beads to over 6.0 for some metallic fillers, but most (including ferrites) occur in 1.6–2.8 range, while common polymers falls in the range from 0.9 to 1.4.[118]

### B. Glass transition temperature ($T_g$)

$T_g$ is developed as a result of cooling of material from cure temperature to room temperature. If cooling is very fast, it will result in nonequilibrium phases and stresses will result. This will result in a lowering of $T_g$. This happens as crystal structures (facets, platelets, globules, spherullites, kinks, bands, whiskers) formed in the matrix tend to coalesce with each other resulting in attainment of liquid state much earlier than in normal pure single phase material due to presence of these stresses.[66] This is a unique phenomenon which is highly anisotropic and must be controlled via careful means to factor against detrimental effects. This is even more prominent and important in the case of magnetic polymers as hybrid (two) composites exist simultaneously and the possibility of formation of stresses and differential stress induced regions is very high as compared to single phase material. Glass transition temperature is also an important function of cure temperature and usually has directly proportional relationship with it. It is measured by differential scanning calorimetry (DSC), and by dynamic mechanical

https://doi.org/10.1557/jmr.2017.63 Published online by Cambridge University Press

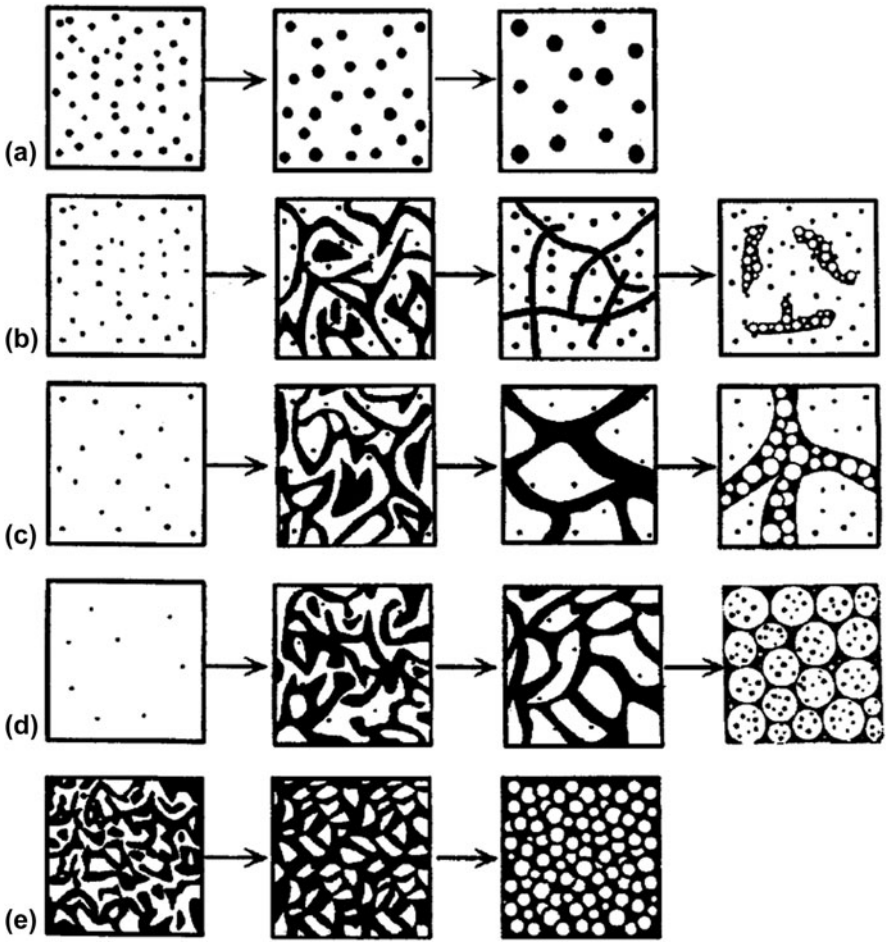



FIG. 7. Model for the morphology formation during curing of thermoplastic/thermoset blend (a) NG only (b) NG followed by SD (dispersed thermoplastic rich phase) (c) NG followed by SD (bicontinuous), (d) NG followed by SD (dispersed thermoset rich phase) and (e) SD only.[115]

thermal analysis (DMTA). Values in second heating run in case of DSC are reported to be $T_g$ while storage modulus, loss modulus, and loss factor, tan δ were calculated as a function of temperature over a temperature range. $T_g$ is reported to be value at which maximum tan δ occurred.

### C. Thermal conductivity

Thermal conductivity may be defined as steady state heat that will be transmitted by a material of given thickness ($t$) and temperature differential ($\Delta t$) per unit area ($A$). This is important in determining the affectivity of material to act as thermal barrier. A material of poor thermal conductivity cannot serve as good heat insulator and vice versa. In magnetic polymer composites, it is of importance when these class of materials are to be subjected to extreme external applications such as parts near engine of aircrafts, parts under the action of friction (rotational or translational), and parts which are under the action of constant exposure to heated surfaces (such as refrigeration and air conditioning parts inside aircraft). Composites reinforced with particles and fibers both show different thermal conductivity behavior. In general, thermal conductivity increases with increase of temperature. This increase is more profound in the case of fibers than in the case of particles if considered separately, because fibers can create networks much easier as particles. In case of pure ferrite particulate reinforced composites, however, this effect is very dominant after percolation threshold. This is because; at this stage particles are linked to make a network so an appreciable change in thermal conductivity is observed. Overall, lower thermal conductivity of particulate reinforced composites is attributed to agglomeration of particles and skin core effect. The higher thermal conductivity of fiber-reinforced composites is also due to higher aspect ratio. Overall for a hybrid composites (such as ours) thermal conductivity increases with increase of filler content (Fig. 8).[117]

### D. Coefficient of thermal expansion (α)

In simplest terms, it can be defined as the rate at which material changes its volume on heating or cooling. It is represented by α. Its SI units are $K^{-1}$. Usually the

https://doi.org/10.1557/jmr.2017.63 Published online by Cambridge University Press

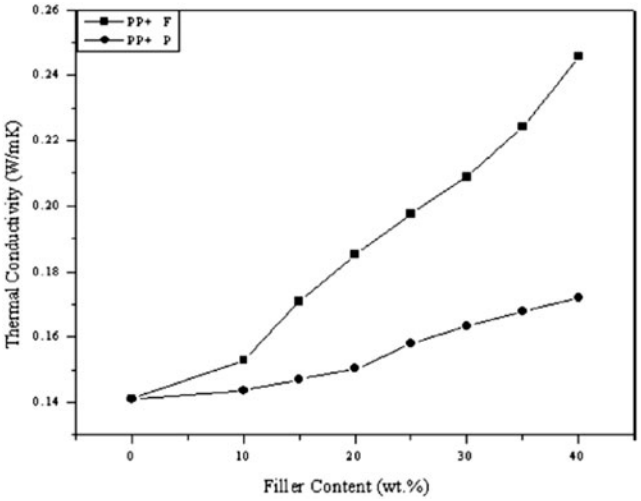



FIG. 8. Thermal conductivity of pure polypropylene and PP composites with particles and fibers as reinforcements.[117]

coefficient of thermal expansion of a particulate filled composite is lower than of the neat polymer resin used as matrix. This is due to the fact interactions between mineral filler particles and polymeric chains result in regions which achieve softening much earlier than the original untempered polymeric chains structure of matrixes due to presence of defects thus reduce the ability of the material to exhibit expansion under the action of heat. In well annealed systems, the rule of mixture applies unless there exists a strong bonding between filler and polymer. Some fillers have a negative coefficient of thermal expansion and are used to achieve composites with zero expansion. Others have anisotropic properties and develop composites which are highly direction dependent with respect to their coefficient of thermal expansion (desirable in MPMC as well).[118]

## E. Electrical properties

In general, pure unfilled polymers are nonconductors/insulators of electricity. There are few intrinsic polymers which are conductive (e.g., polyaniline, polypyrole, and polythiophene) but they are rare and expensive.[118] The introduction of conductive nano-inorganic particle in an isolating polymer matrix beyond percolation threshold imparts the electrical properties of the composite. Generally this percolation threshold is considered to be lower for fibers (high aspect ratio) as compared to spherical particulates (ferrites). A re-agglomeration of nanotubes will lead to conductive paths at lower filler contents in relation to aspect ratio and mobility in the matrix. Electrical conductivity of composites arises from conductive paths, already present or developed as a result of inclusion of foreign particles in matrix (Fig. 9).[119]

Nonfunctionalized DWCNTs have the highest tendency to re-agglomerate under formation of conductive paths. Its percolation threshold has been determined to be below 0.1 wt%. Water pickup is another property which determines the behavior of molecule or material to behave toward matrix in a conductive or nonconductive manner. A more reactive surface (such as of meta-kaolin) helps in increasing the electrical performance of composite. Another important property is tracking (build-up of surface charge and its release (discharge) across the surface). Due to their good insulation characteristics, this phenomenon is very much prevalent in thermoplastics. Inclusions of inorganic filler particles (ferrites) result in a change (reduction) of the path through which discharge should occur thus reducing this problem. Ability of polymers to act as insulators also results in build-up of static charge on their surfaces which leads toward accumulation of dust in such places as well. This is especially prominent in the case of surfaces which are narrow and covered by a lot of high "length to diameter" components (e.g., transistors, capacitors). Sometimes, a sufficiently high conductivity is needed. It is predominant in the case of electromagnetic interference (EMI) shielding and is particularly true in case of soft magnetic polymers (described in Sec. I above).

## F. Mechanical properties

This is a field which is given very high interest in terms of research and development of polymer matrix composites. So, here we will present a comprehensive treatment of the subject outlining and explaining all the mechanisms involved and processes behind origin and development of mechanical properties in composites with particular focus on magnetic polymer matrix composites (MPMCs). We start with the very basic inherent nature of polymers and then will proceed to advanced concepts. Mechanical properties of thermoplastics and thermosets result from a combination of fiber and matrix properties and the ability to transfer stresses across fiber/matrix interface.[68] Key factors such as interfacial adhesion, fiber length-to-diameter ratio and concentration, matrix ductility, residual stresses (due to a difference in coefficient of thermal expansion between fiber and matrix) and induced stresses (as a result of mechanical working, service history, and curing) determine complex fracture mechanics behavior. Other factors such as porosity, voids[64] also dictate mechanical properties.[63]

## G. Intrinsic deformation

It was in 1965 that Haward and Thackray[120] described the materials response with two parallel processes. (i) Initial nonlinear elastic response up to yield (controlled by secondary intermolecular interactions) combined with (ii) entanglement network response in

https://doi.org/10.1557/jmr.2017.63 Published online by Cambridge University Press

parallel from the primary intramolecular interactions which gives entropic contributions at large strains. Several groups worldwide discussed these processes including Mary Boyce (MIT),[121,122] Paul Buckley (Oxford)[123–125] and Han Meijer (TU/e Eindhoven).[126–128] As a whole, they used rubber elasticity to model "strain hardening" and stress dependent viscosity to capture "deformation kinetics". As is the case with temperature, an applied stress leads to increase in segmental mobility which consequently results in a decrease in viscosity (shear induced viscosity). In extreme cases, this leads to yielding, the onset of flow, induced by stress (stress induced glass transition).

It was also shown by Doros Theodorou and Uli Suter at MIT[129] via ab-initio calculations that affine deformations along the chain do not exist outside a region of roughly 10 carbon atoms. This is very much true even today to indicate the process of plastic deformations in amorphous polymers i.e., relating it to molecular motion on segmental scale. Only secondary interactions and free volume kinetics are of primary interest and play a pivotal role before critical stress. Once the critical stress is surpassed, the stress to further flow should be constant, until the entanglement network starts to orient. In this region, it is the entanglement that controls the modulus and it is the molecular weight that controls the strength at breakage. Another property of interest is "noncatastrophic localization". This can [in case of bullet proof polycarbonate (PC)] and cannot [brittle polystyrene (PS)] occur and are explained in terms of strain softening followed by strain hardening at large deformations (Fig. 10).

Mechanical rejuvenation in high entanglement polymers can be observed at low cyclic loadings (just simple to and from motion of a thin specimen) and low filler loadings. It is conceived that once secondary bonds are locally weakened by stress, the material must flow under a constant stress up to a point that strain hardening sets in. That is exactly what is observed in rejuvenated materials. It is also observed that the density of materials increases during this rejuvenation process.

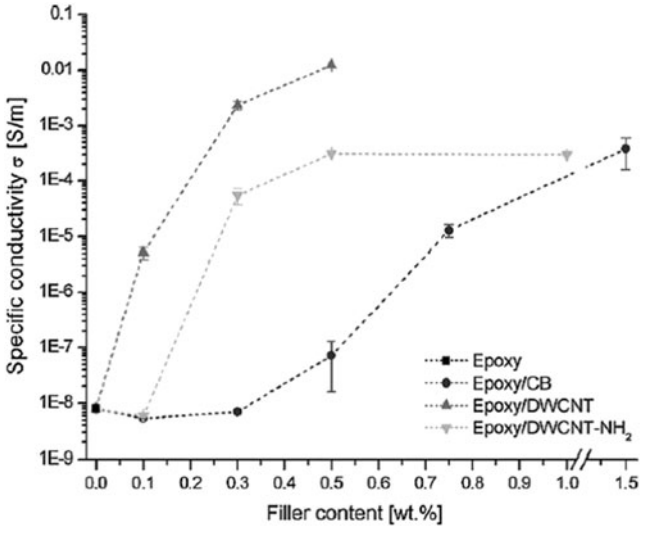



FIG. 9. Electrical conductivity of the nanoparticle reinforced epoxy resin (at $f = 1000$ Hz).[119]

## H. Tensile/Young's modulus

After the onset of intrinsic deformation, material yields. The phenomena during this stage can be explained by physical aging, yielding, and elongation under tensile stress to failure. If segmental mobility is increased by stress rather than by temperature, a growing peak in stress in a stress–strain curve is observed that can be interpreted toward the increase in yield stress followed by softening (discussed later) and can be credited toward property known as Tensile/Young's Modulus.[62,65] It was observed that tensile modulus increases with the increase of filler content. This is expected because the Young's modulus of fillers (ferrites) embedded in epoxy (our case) is much higher than the parent neat epoxy resin. The simplest explanation of this can be given by three of main known models "rule of mixture", "Halpin–Tsai" and "Mori–Tanaka" relationships. These are based on a number of assumptions such as

(i) Matrix and the particles are considered to be linear-elastic, isotropic.

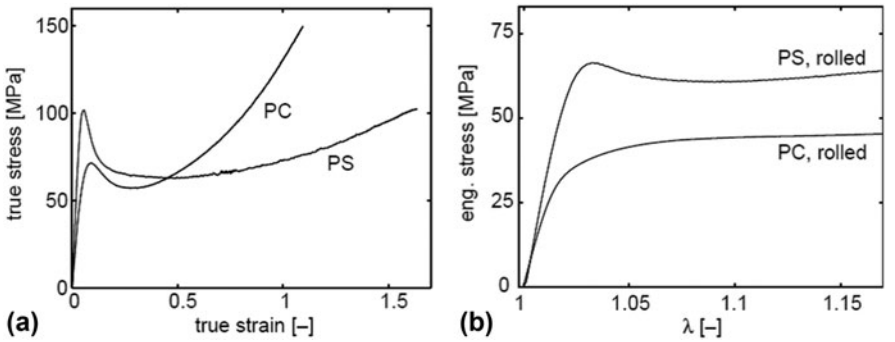



FIG. 10. Intrinsic behavior of polycarbonate (PC) and polystyrene (PS) before (a) and after (b) mechanical rejuvenation.[129]



https://doi.org/10.1557/jmr.2017.63 Published online by Cambridge University Press

(ii) There is perfect bonding between the particles and the matrix.

(iii) The particles are (where applicable) uniform in their aspect ratio.

(iv) Particles are perfectly aligned with the applied load.

(v) Any agglomeration and particle–particle interactions are ignored.

In general the rule of mixture gives very poor results.[130] The Mori–Tanaka model is a good approximation of actual conditions but it suffers from the drawback that it is only valid and yields good result for high aspect ratio fillers. As the aspect ratio reaches unity (spherical particles) it predicts a negligible reinforcing effect which is not desired in present discussion.[131,132] A very good approximation is given by Halpin and Tsai who explained the occurring of yield modulus of composites in terms of modulus of matrix polymer, that of filler particle and a shape factor. The modified modulus is given by

$$E_c = \frac{1 + \zeta \eta V_f}{1 - \eta V_f} E_m \quad . \tag{10}$$

A detailed explanation and comprehensive treatment of this young's modulus is given in original paper of Halpin and Tsai of 1969.[133,134]

## I. Crack pinning

Primarily, toughening mechanisms can be broadly classified into on-plane (crack pinning or bowing and crack deflection) or off plane processes (debonding and plastic void growth). Crack pinning mechanisms have been invoked for micrometer sized particles and also for nanoparticles. These are the predominant mechanisms of operation in case of metals and alloys. For polymers, reinforced with particles (PRC) and then PRC reinforced hybrid GFRP, this mechanism has been very recently exploited. "Bowing lines" which are characteristic of the onset of the occurring of crack pinning by dislocations, are observed in epoxies.[135] Another geometrical feature/property known as crack opening displacement (COD) is used to explain this. If the particles are larger than COD, this is an indication of the onset of crack pinning and vice versa. This is because, for particles larger than COD, dislocations tend to bow in spaces between particles, increasing its length and energy required for deformation. COD can be mathematically calculated and can be used for the determination of the onset of crack pinning or otherwise. It is assumed that, based on prior observations from particles of similar size[136] that ferrite particles in nanosize would not be effective in causing an increase in toughness of composites from crack pinning phenomena.

## J. Crack deflection

Toughening in composites could be due to crack deflection processes when the crack front tilts and twists upon its encountering the particle and hence passes through them. This causes an increase in total fracture surface area and also causes the crack to grow locally under mixed–mode I/II conditions. The former toughening effect can be measured by comparing the measured fracture toughness with the surface roughness while latter effect can be evaluated by the use of a method devised by Faber and Evans.[137] There are other mechanisms such as immobilized polymers, plastic void growth which can effectively explain the underlying phenomena responsible for the defects, cracks, their development, progression and increase in toughness (impact resistance) in particulate reinforced polymer composites (PRC) in general and can be used toward fiber reinforced magnetic polymer matrix composites in particular. The treatment of these is beyond the scope of present work and can be found in dedicated literature for this purpose.[118,136,138,139]

## K. Magnetic properties

Magnetic properties of polymers are highly size dependent and care should be taken to choose and control the process to get optimum results. Usually elements responsible for imparting magnetic properties are used in their compound shape and never in their virgin (unreacted) state. For example Fe is used as $Fe_2O_3$ or $Fe_3O_4$ but never as Fe as it will oxidize instantaneously.

## L. Magnetoelasticity

The elastic properties of magneto composites are field dependent. This is an extremely important property of polymers which determine their preferential/directional alignment under the action of applied field if loaded with magnetic responsive particles. In a uniform field, a magnetoelastic experience no field but the magnetic particles are aligned. In a magnetic gradient, however, the particles are attracted by the stronger field and move along with the polymer resulting in a large macroscopically visible deformation of the body. This is of special interest to prepare composites which with pre-realigned particles bear inherent anisotropic properties (partial objective of present research). This can be achieved by preparing composites in the presence of magnetic field at the stage of mixing. Thus in a magnetic field the elastic modulus is dependent on the orientation of the polymer block with respect to the direction of magnetic field vector. The application areas for these materials are smart sensors and actuators.[141]

## M. Microwave magnetic guidance

These are magnetic nanocomposites materials which make use of microwave radiation to exploit

https://doi.org/10.1557/jmr.2017.63 Published online by Cambridge University Press

bonding–debonding on two different parts. For example, microwave absorption of spin wave excitation in Ni–Zn Ferrites in contact with a heat sensitive adhesive is used as bond/disbond-on-command. However, a disadvantage associated with this technique is that it requires preferential direction of microwave radiation at a specific area which requires the development of special tooling and fixtures to achieve the result. Another being the inherent dangerous nature of microwaves causing heat and burn. This necessitates the use of protective gloves and apparel.[140]

## N. *B–H* curve (hysteresis loop)

Remanence (remanent induction or residual flux density) and coercive force (coercivity) of polymer magnetic composites are determined from *B–H* curve. A SQUID type vibrating sample magnetometer (VSM) is used for determination of *B–H* curve at room (present case) or elevated temperature. As can be observed from figures [Figs. 11(a)–11(f)] below that remanence increased while coercive force decreased (long thin *B–H* curves) with increase of filler content in particle reinforced composites (PRC) in all three cases of Ba, Sr (isotropic) and anisotropic ferrites. Further, this trend is linear in both cases. It could be attributed to the fact that the lesser force is required to take the value of residual magnetization to zero if a larger number of particles is present in a given volume. Under similar conditions, the same large number of particles will result in higher values of remanence (remanent induction) because it will make the material a stronger magnet.

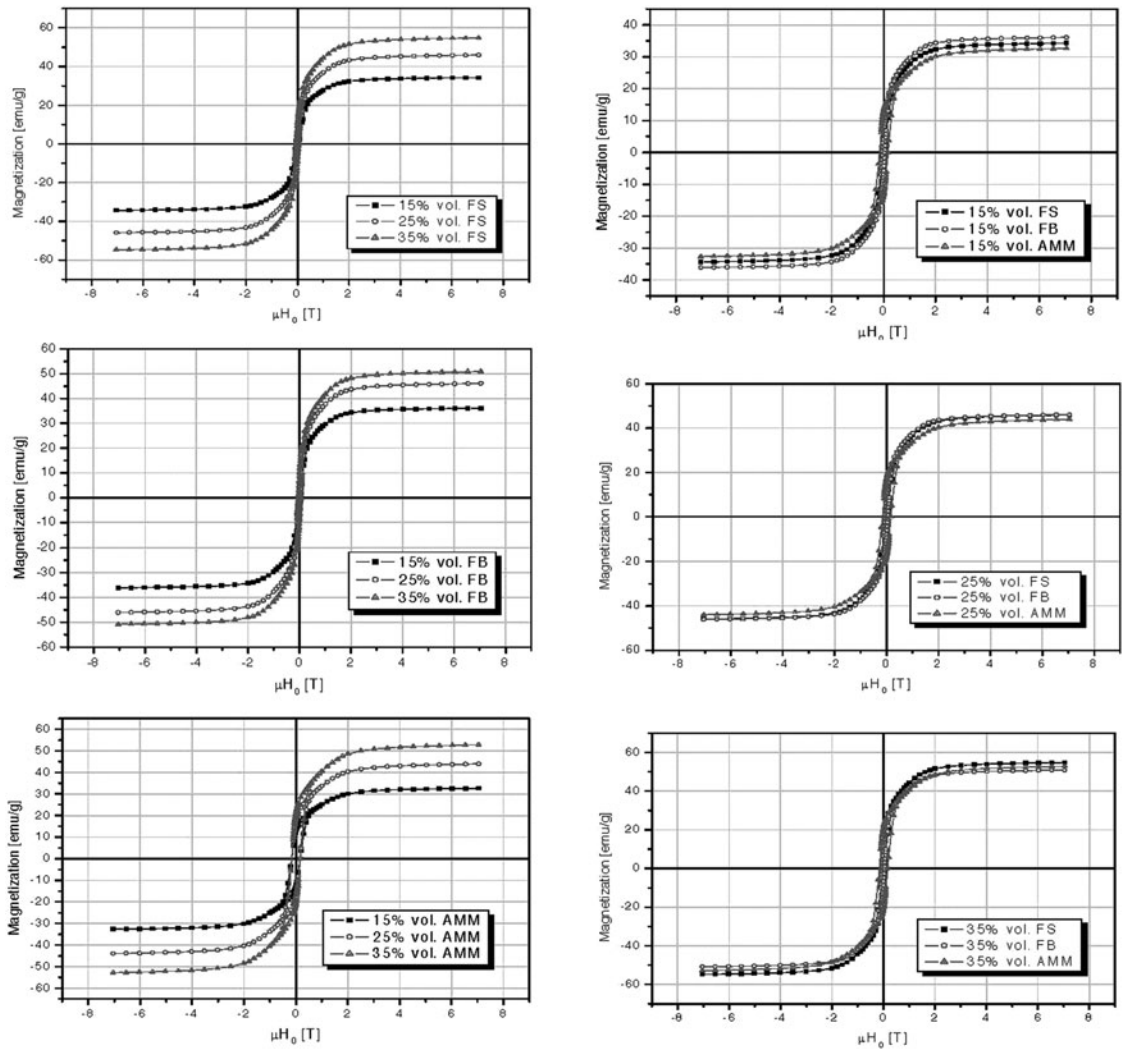



FIG. 11. (a)–(f) Hysteresis loop of polymer magnetic composite materials with different types and volume percentages of fillers. (a) 15, 25 and 35 vol% of Sr ferrite isotropic particles (b) 15 vol% of Br, Sr (isotropic) and anisotropic material (c) 15, 25 and 35 vol% of Br ferrite isotropic particles (d) 25 vol% of Br, Sr (isotropic) and anisotropic material (e) 15, 25 and 35 vol% of anisotropic material (f) 35 vol% of Br, Sr (isotropic) and anisotropic material.[44]



https://doi.org/10.1557/jmr.2017.63 Published online by Cambridge University Press

This effect (variation of remanence and coercivity) is same in case of isotropic (randomly oriented) particles while composite materials with anisotropic filler have much higher values for remanence and coercivity (about two times higher for remanence and three times higher for coercive force). The highest value of remanence is 21 [emu/g] and was obtained for sample with 35 vol% of anisotropic powder amount whereas the lowest value is 13 [emu/g] for 15 vol% of anisotropic material. The highest remanence for composite material with 35 vol% of strontium ferrite is 9 [emu/g], while with 35 vol% of barium ferrite, it is 8.7 [emu/g]. Coercive force for composite material with 35 vol% anisotropic filler measures 118 [kA/m], while for 15 vol% of anisotropic material, it is 127 [kA/m]. The highest value of coercive force for composite materials with isotropic filler was obtained for 15 vol% of strontium ferrite and it was 37.8 [kA/m].[44]

## O. Magnetic induction, susceptibility, and saturation induction

In another study, Ali Ghasemi and co-workers[141] embedded polymer composites with tin doped strontium ferrite nanoparticles and studied their structural and magnetic characteristics. They varied the composition of doped strontium ferrite ($SrFe_{12-x}Mg_{x/2}Sn_{x/2}O_{19}$) as a function of $x$ (1, 2, and 3) and presented excellent results in terms of $x$ values.

The coercivities were obtained from demagnetization curves. Whereas, intrinsic magnetic parameters such as magnetic anisotropy field ($H$)/magnetic induction ($B$) and high field susceptibility $\chi_p$ were deduced from numerical analysis of magnetization curves based on the law of approach to saturation. They showed [Fig. 12(b)] that the values of coercivities and anisotropy field [magnetic induction ($B$)] depends on Mg–Sn substitution as represented by variation of x varied at ambient temperature. Clearly, it is indicative that coercivities decrease linearly from 130 Oe for $x = 1$ to 85 Oe for $x = 3$. A similar trend is observed for an anisotropic field. However, the trend is not as steep as is in the case of coercivity. The reasons for this effect could be attributed again to a large number of particle resulting in accumulation of higher values of net magnetic field with increasing values of $x$ which removes the necessity of the use of higher negative magnetic fields (demagnetization) to achieve values of residual magnetization to zero. A different plot [Fig. 12(c)] shows high field susceptibility $\chi_p$ as a function of Mg–Sn content at room temperature and depict that a different behavior is observed. The value of $\chi_p$ increase rapidly from $x = 1$ to $x = 3$. The value of susceptibility of sample with $x = 3$ is doubly large than sample with $x = 1$. The saturation magnetization, on the other hand, decreases with increase of $x$. This can also be observed in full hysteresis loop ($B$–$H$ curve) [Fig. 12(a)]. This effect can be attributed to the fact that above $x > 1$ non collinear magnetic structure (spin canting) exists. The similar behavior was observed on doping with other elements.[142] In a later study, Shimba, Kazuaki et al.,[143] studied the effect of soft ferrites on magnetic properties of polymer composites prepared using surface modifiers and crosslinkers. They separately prepared nanoparticles

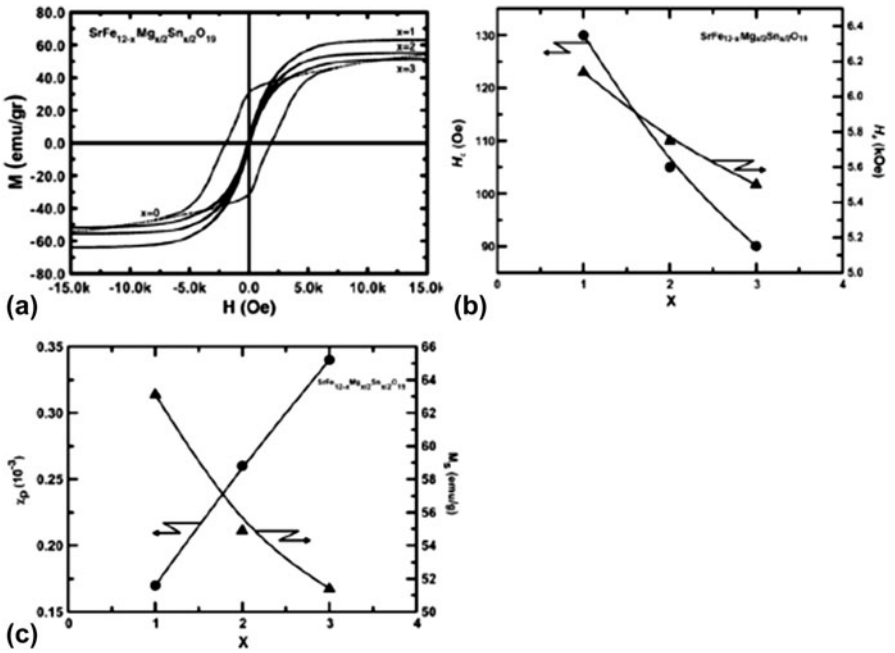



FIG. 12. Magnetic properties of doped Sr ferrites (a) hysteresis loop ($B$–$H$ curve) with different concentrations of dopants (b) variation of coercivity and anisotropic field with $x$ (c) high field susceptibility ($\chi_p$) and saturation magnetization as a function of $x$.[141]



https://doi.org/10.1557/jmr.2017.63 Published online by Cambridge University Press

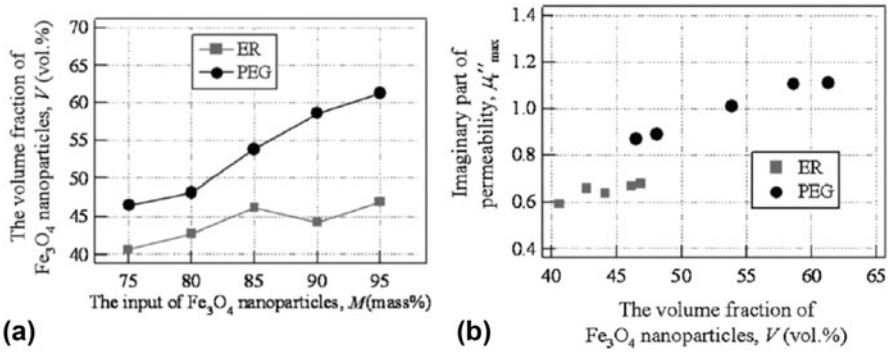



FIG. 13. (a) Volume fraction of $Fe_3O_4$ nanoparticles ($V$) as a function of mass fraction ($M$) (b) imaginary part of permeability $\mu_r''$ as a function of volume fraction ($V$) of $Fe_3O_4$ nanoparticles.[143]

by coprecipitation reaction and then prepared composites following surface modification and crosslinking reactions. 4-META (4-methacryloylioxyethyl trimelliate anhydride) was used as surface modifier while PEG–4SH (pentaerythritol tetra–polyethylene glycol ether with four thiol-modified terminals) was used as cross linker. For comparison with microwave absorption properties of PEG composite, a conventional epoxy resin (ER) composite was also fabricated. Variation of volume fraction of nanoparticles expressed as volume percentage $V$ (vol%) is plotted as a function of mass percentage $M$ (mass%) and is shown in Fig. 13(a).

It can be easily seen that for all cases, $V$ is larger for PEG composite than for ER composite at same value of $M$, and $V$ for PEG increases with $M$ until reaching a maximum of 62% at $M = 95\%$. Hence they showed that the volume fraction of magnetic particles in a composite can be increased by using nanoparticles processed with surface modifiers and crosslinkers (as mass fraction increases with later treatments). A similar treatment of plotting relative permeability as a function of volume fraction resulted in Fig. 13(b). It was observed that for each value of $V$, the imaginary part of relative permeability $\mu_r''$ is consistently higher in PEG composites than in ER composites, and the largest value for PEG is $\mu_{rmax}'' = 1.11$. This happened as $V$ is higher for PEG composites as compared to ER Composites. The consequences and mechanisms behind this can again be directly attributed to a large percentage of particles giving rise to higher values.

## IV. CONCLUSIONS

Ferrites comprise of one of the most important inorganic magnetic materials used as fillers today for achieving magnetic properties in polymer matrix composites. Their use was, however, limited in polymeric matrix composites owing to technical difficulties encountered during the processing (mixing) of ferrites in polymer resins and some inherent disadvantages associated with limiting percentage of ferrites beyond a certain threshold of mixing. This challenge has been overcome efficiently in recent years by application of various mixing techniques employing different technologies (*in situ* polymerization, *ex situ* ultrasonic mixing, magnetic stirring etc.). The present work highlights and ensembles these trends and compiles a review of very recent advances in ferrite technology and its use in making thick fiber-reinforced magneto-polymer matrix composites (MPMCs) as advanced material for aerospace structures. Various phenomena underlying their formation, processing, characterization, and property development are elaborately discussed with aim of reaching optimized magnetic GFRP. Three materials namely, barium, cobalt, and strontium ferrite were tested and examined for their suitability and application in polymer resins for developing magnetic properties for aerospace structures. Although, the general trend for research on cobalt ferrite is high, for aerospace applications, barium ferrite was proposed as strong candidate as it is easy to mix in polymeric resins, has a high resolution under an electron microscope, shows superior mixing properties when mixed in low to moderate amounts in polymer resins—which is required for achieving optimum viscosity without sacrificing mechanical (yield and ultimate tensile) strength and exhibits excellent response to an applied magnetic field with retention of magnetism even after removal of the field.

## REFERENCES

1. D. Halliday, R. Resnick, and K. Krane: *Fundamentals of Physics*, 9th ed. (John Wiley and Sons, New York, 2011).
2. K.H.J. Buschow and F.R. de Boer: *Physics of Magnetism and Magnetic Materials* (Kluwer Academic/Plenum Publishers, New York, 2004).
3. A. Goldman: *Modern Ferrite Technology*, 2nd ed. (Springer Science + Business Media, Inc., Pittsburgh, 2006).
4. J. Smit and H.P.J. Wijn: Ferrites. In *Philips Technical Library* (N. V. Philips, Gloeilampenfabrieken, Eindhoven, 1959).
5. E.E. Riches: *Ferrites* (Mills and Boon Limited, London, 1972).

https://doi.org/10.1557/jmr.2017.63 Published online by Cambridge University Press

6. M.G. Say: *Magnetic Alloys and Ferrites* (George Newns Limited, London, 1954).
7. R.C. Pullar: Hexagonal ferrites: A review of the synthesis, properties and applications of hexaferrite ceramics. *Prog. Mater. Sci.* **57**, 1191–1334 (2012).
8. P. Martins, Y.V. Kolen'ko, J. Rivas, and S. Lanceros-Mendez: Tailored magnetic and magnetoelectric responses of polymer-based composites. *ACS Appl. Mater. Interfaces* **7**, 15017–15022 (2015).
9. H. Sozeri, U. Kurtan, R. Topkaya, A. Baykal, and M.S. Toprak: Polyaniline (PANI)–$Co_{0.5}Mn_{0.5}Fe_2O_4$ nanocomposite: Synthesis, characterization and magnetic properties evaluation. *Ceram. Int.* **39**, 5137–5143 (2013).
10. T. Khursheed, M.U. Islam, M.A. Iqbal, I. Ali, A. Shakoor, M.S. Awan, A. Iftikhar, M.A. Khan, and M.N. Ashiq: Synthesis and characterization of polyaniline–hexaferrite composites. *J. Magn. Magn. Mater.* **393**, 8–14 (2015).
11. D. Puryanti, S.H. Ahmad, and H.A. Mustaffa: Effect of nickel–cobalt–zinc ferrite filler on electrical and mechanical properties of thermoplastic natural rubber composites. *Polym.-Plast. Technol. Eng.* **45**, 561–567 (2006).
12. K. Praveena, K. Sadhana, and S.M. Ramana: Structural and magnetic properties of NiCuZn ferrite/$SiO_2$nanocomposites. *J. Magn. Magn. Mater.* **323**, 2122–2128 (2011).
13. P. Raju, T. Ramesh, and S.R. Murthy: Ferrite + polymer nanocomposites for EMI applications. *Int. J. ChemTech Res.* **7**(3), 1343–1350 (2015).
14. S. Chen, S. Chen, G. Zhao, and J. Chen: Fabrication and properties of novel superparamagnetic, well-dispersed water-borne polyurethane/Ni–Zn ferrite nanocomposites. *Compos. Sci. Technol.* **119**, 108–114 (2015).
15. C. Wang, Y. Niu, P. Pei, Y. Shen, H. Zhang, and A. Xie: Synthesis, characterization and dielectric properties of polyaniline@$Ni_{0.5}Zn_{0.5}Fe_2O_4$ composite nanofibers. *Mater. Sci. Semicond. Process.* **40**, 140–144 (2015).
16. Y. Xie, X. Hong, X. Wang, J. Zhao, Y. Gao, Y. Ling, S. Yan, L. Shi, and K. Zhang: Preparation and electromagnetic properties of La-doped barium–ferrite/polythiophene composites. *Synth. Met.* **162**, 1643–1647 (2012).
17. Y. Xie, X. Hong, Y. Gao, M. Li, J. Liu, J. Wang, and J. Lu: Synthesis and characterization of La/Nd-doped barium–ferrite/polypyrrole nanocomposites. *Synth. Met.* **162**, 677–681 (2012).
18. L. Chen and G. Xing-long: Damping of magneto rheological elastomers. *J. Cent. South Univ.* **15**(1), 271–274 (2008).
19. M. Kallio: *The Elastic and Damping Properties of Magneto-rheological Elastomers*, Vol. **565** (VTT Publications, Espoo, 2005); p. 146.
20. A.P.P. Fulco, J.D.D. Melo, C.A. Paskocimas, S.N. Medeiros, F.L.A. Machado, and A.R. Rodrigues: Magnetic properties of polymer matrix composites with embedded ferrite particles. *NDT&E Int.* **77**, 42–48 (2016).
21. G. Andrei, D. Dima, L.G. Birsan, and A. Circiumaru: Effect of ferrite particles on mechanical behaviour of glass fibre reinforced polymer composite. *Mater. Plast.* **46**(3), 284–287 (2009).
22. D. Dima and G. Andrei: Investigation of the effect of $Fe_3O_4$ particles on the interface of Gf–Pr–Fa magnetic composites. *Materialwiss. Werkstofftech.* **34**, 349–353 (2003).
23. M.R. Kessler, N.R. Sottos, and S.R. White: Self-healing structural composite materials. *Composites, Part A* **34**, 743–753 (2003).
24. R.S. Trask, H.R. Williams, and I.P. Bond: Self-healing polymer composites: Mimicking nature to enhance performance. *Bioinspiration & Biomimetics* **2**, 1–9 (2007).
25. I.P. Bond, R.S. Trask, H.R. Williams, and G.J. Williams: *Self-healing Fibre-reinforced Polymer Composites: An Overview, in Self-healing Polymers*, S. van der Swaag, ed. (Springer Publishing, Houten, 2015).
26. A.V. Bychkova: Magnetic and transport properties of magneto-anisotropic nanocomposites for controlled drug delivery. *Nanotechnol. Russ.* **10**(3–4), 325–335 (2015). [in Russian].
27. T. Gundermann, S. Günther, D. Borin, and S. Odenbach: A comparison between micro- and macro-structure of magneto-active composites, 13th Int. Conf. on Electrorheological Fluids and Magnetorheological Suspensions (ERMR2012). *J. Phys.: Conf. Ser.* **412**, 012027 (2013).
28. I. Bica, E.M. Anitas, and L.M.E. Averis: Tensions and deformations in composites based on polyurethane elastomer and magnetorheological suspension: Effects of the magnetic field. *J. Ind. Eng. Chem.* **28**, 86–90 (2015).
29. A. Boczkowska, S.F. Awietjan, S. Pietrzko, and K.J. Kurzydłowski: Mechanical properties of magnetorheological elastomers under shear deformation. *Composites, Part B* **43**, 636–640 (2012).
30. A. Boczkowska and S. Awietjan: Intelligent magnetorheological elastomer composites. *Polimery* **58**(6), 443–449 (2013).
31. J. Li, X. Gong, H. Zhu, and W. Jiang: Influence of particle coating on dynamic mechanical behaviors of magnetorheological elastomers. *Polym. Test.* **28**, 331–337 (2009).
32. X. Qiao, X. Lu, X. Gong, T. Yang, K. Sun, and X. Chen: Effect of carbonyl iron concentration and processing conditions on the structure and properties of the thermoplastic magnetorheological elastomer composites based on poly(styrene-*b*-ethylene-*co*-butylene-*b*-styrene) (SEBS). *Polym. Test.* **47**, 51–58 (2015).
33. Y. Zhou: The influence of particle content on the equi-biaxial fatigue behaviour of magnetorheological elastomers. *Mater. Des.* **67**, 398–404 (2015).
34. M.Y. Razzaq, M. Behl, and A. Lendlein: Magnetic memory effect of nanocomposites. *Adv. Funct. Mater.* **22**, 184–191 (2012).
35. J. Thévenot, H. Oliveira, O. Sandre, and S. Lecommandoux: Magnetic responsive polymer composite materials. *Chem. Soc. Rev.* **42**, 7099 (2013).
36. A. Grujić, N. Talijan, D. Stojanović, J. Stajić-Trošić, Z. Burzić, L.j. Balanović, and R. Aleksić: Mechanical and magnetic properties of composite materials with polymer matrix. *J. Min. Metall., Sect. B* **46**(1), 25–32 (2010).
37. G. Andrei, D. Dima, L.G. Bîrsan, and L. Andrei: Improving the properties of new magnetic composite with polyester resin matrix. In *Proc. of ROTRIB'03, National Tribology Conference, Galati, The annals of the university "Dunarea de Jos" of Galati, Fascicle VIII: Tribology* (2003); pp. 124–128.
38. D. Dima and O. Mitoseriu: The use and behaviour of composite materials with particles when obtaining rolls for rolled sheet iron oiling plant. In *Proc. of ROTRIB'03, National Tribology Conference, Galati, The annals of the university "Dunarea de Jos" of Galati, Fascicle VIII: Tribology* (2003); pp. 115–117.
39. G. Andrei, D. Dima, and L. Andrei: Lightweight magnetic composite for aircraft applications. *J. Optoelectron. Adv. Mater.* **8**(2), 726–730 (2006).
40. E. Goiti, R. Hernandz, R. Sanz, D. Lepez, M. Vazquez, C. Mijangos, R. Turcu, A. Nan, D. Bica, and L. Vekas: Novel nanostructured magneto polymer composite. *Nanostruct. Polym. Nanocompos.* **2**, 5–12 (2006).
41. C. Adrian, A. Gabriel, G.B. Iulian, and A. Semenescu: Electrical conductivity of fabric based filled epoxy composites. *Mater. Plast.* **46**(2), 211–214 (2009).
42. D. Dima: Research on polymeric composite materials with particles using comparative tests. *Acad. J. Manufact. Eng.* **8**(1), 43–48 (2010).
43. J. Stabik, A. Dybowska, J. Pluszynski, M. Szczepanik, and L. Suchon: Magnetic induction of polymer composites filled with ferrite powders. *Arch. Mater. Sci. Eng.* **41**(1), 13–20 (2010).


https://doi.org/10.1557/jmr.2017.63 Published online by Cambridge University Press

44. J. Stabik, A. Chrobak, G. Haneczok, and A. Dybowska: Magnetic properties of polymer matrix composites filled with ferrite powders. *Arch. Mater. Sci. Eng.* **48**(2), 97–102 (2011).
45. J. Stabik, A. Dybowska, and M. Chomiak: Polymer Composites filled with powders as polymer graded materials. *J. Achiev. Mater. Manufact. Eng.* **43**(1), 153–161 (2010).
46. J. Stabik, A. Dybowska, M. Szczepanik, and L. Suchon: Viscosity measurement of epoxy resin filled with ferrite powders. *Arch. Mater. Sci. Eng.* **38**(1), 34–40 (2009).
47. L.A. Dobrzanski and M. Drak: Structure and properties of composite materials with polymer matrix reinforced Nd–Fe–B hard magnetic nanostructured particles. *J. Mater. Process. Technol.* **157–158**, 650–657 (2004).
48. L.A. Dobrzanski and M. Drak: Properties of composite materials with polymer matrix reinforced with Nd–Fe–B hard magnetic particles. *J. Mater. Process. Technol.* **175**, 149–156 (2006).
49. M. Drak and L.A. Dobrzanski: Hard magnetic materials Nd–Fe–B/Fe with epoxy resin matrix. *J. Achiev. Mater. Manufact. Eng.* **21**(2), 63–66 (2007).
50. B. Ziebowicz, D. Szewieczek, and A.L. Dobrazanski: Magnetic properties and structure of nanocomposites of powder $Fe_{73.5}Cu_1Nb_3Si_{13.5}B_9$ alloy—Polymer type. *J. Mater. Process. Technol.* **157–158**, 776–780 (2004).
51. D. Szewieczek, A.L. Dobrzański, and B. Ziebowicz: Structure and magnetic properties of nanocomposite of nanocrystalline powder—Polymer type. *J. Mater. Process. Technol.* **157–158**, 765–770 (2004).
52. B. Ziebowicz, D. Szewieczek, A.L. Dobrzanski, J.J. Wysłocki, and A. Przybył: Structure and properties of composite materials consisting of the nanocrystalline $Fe_{73.5}Cu_1Nb_3Si_{13.5}B_9$ alloy powders and polyethylene. *J. Mater. Process. Technol.* **162–163**, 149–155 (2005).
53. L.A. Dobrzański, M. Drak, and B. Ziebowicz: New possibilities of composite materials applications – materials with specific magnetic properties. *J. Mater. Process. Technol.* **191**, 352–355 (2007).
54. L.A. Dobrzański, A. Tomiczek, B. Tomiczek, A. Ślawska-Waniewska, and O. Iesenchuk: Polymer matrix composite materials reinforced by $Tb_{0.3}Dy_{0.7}Fe_{1.9}$ magnetostrictive particles. *J. Achiev. Mater. Manufact. Eng.* **37**(1), 16–23 (2009).
55. L. Valko, P. Bucek, R. Dosoudil, and M. Usakova: Magnetic properties of ferrite polymer composites. *J. Electr. Eng.* **54**(3–4), 100–103 (2003).
56. J. Rekošová, R. Dosoudil, M. Ušáková, E. Ušák, and I. Hudec: Magneto polymer composites with soft magnetic ferrite fillers. *IEEE Trans. Magn.* **49**(1), (2013).
57. J. Rekosova: The influence of soft magnetic fillers on the properties of magneto polymer composites, Contributed Lecture (CL) 18. *Chem. Listy* **107**, s40–s100 (2013).
58. J.M. Cuevas, J. Alonso, L. German, M. Iturrondobeitia, J.M. Laza, J.L. Vilas, and L.M. León: Magneto-active shape memory composites by incorporating ferromagnetic microparticles in a thermo-responsive polyalkenamer. *Smart Mater. Struct.* **18**, 075003 (2009).
59. A. Kumar and B. Bhattacharya: Real time integrity monitoring of composite laminates with magnetostrictive sensory layer. In *Proc. SPIE Vol. 7268, Smart Structures, Devices, and Systems IV*, S.F. Al-Sarawi, V.K. Varadan, N. Weste and K. Kalantar-Zadeh, eds. (SPIE, Melbourne, 2008); p. 72680N.
60. A.V. Krishnamurthy, M. Anjanappa, Z. Wang, and X. Chen: Sensing of delaminations in composite laminates using embedded magnetostrictive particle layers. *J. Intell. Mater. Syst. Struct.* **10**, 825–835 (1999).
61. G. Currie, D. Spayde, and O. Myers: Two tiered analysis of CFRP laminate embedded with magnetostrictive particles. In *Proc. of the ASME 2010 Conference on Smart Materials, Adaptive Structures and Intelligent Systems, SMASIS2010*, Vol. 2 (ASME, Philadelphia, 2010); pp. 685–691.
62. J.M. Oliver, G. Currie, and J. Rudd: Tensile testing and non-destructive evaluation scanning of varied ply CFRP laminates with embedded magnetostrictive particles. Presented at the 54th AIAA/ASME/ASCE/AHS/ASC Structures, Structural Dynamics, and Materials Conference (held in Boston, 8–1 April 2013).
63. X. Chen and M. Anjanappa: Health monitoring of composites embedded with magnetostrictive thick film without disassembly. *Smart Mater. Struct.* **15**, 20–32 (2006).
64. J. Rudd, D. Spayde, and O. Myers: Experimental non-destructive testing using magnetostrictive particles embedded in carbon fibre reinforced polymer beams. In *Proc. of the ASME 2012 Conference on Smart Materials, Adaptive Structures and Intelligent Systems SMASIS2012* (ASME, Stone Mountain, 2012); pp. 707–711.
65. O.I. Zhupanska and R.I. Sierakowski: Mechanical response of composites in the presence of an electromagnetic field. Presented at the 46th AIAA/ASME/ASCE/AHS/ASC Structures, Structural Dynamics & Materials Conference (held in Austin, 18–21 April 2005).
66. R.J.C. Carbas, E.A.S. Marques, A.M. Lopes, and L.F.M. da Silva: Effect of Cure temperature on the glass transition temperature of an epoxy adhesive. *J. Adhes.* **90**(1), 104–119 (2013).
67. A. Khomenko, E.G. Koricho, and M. Haq: Monitoring the effect of micro-/nanofillers on curing induced shrinkage in epoxy resins. In *Fillers and Reinforcements for Advanced Nanocomposites* (Elsevier, Amsterdam, 2015); ch. 18.
68. E.G. Koricho, A. Khomenko, and M. Haq: Influence of nano-/microfillers on impact response of glass fibre-reinforced polymer composite. In *Fillers and Reinforcements for Advanced Nanocomposites* (Elsevier, Amsterdam, 2015); ch. 19.
69. F.W. Billmeyer, Jr.: *Textbook of Polymer Science*, 3rd ed. (John Wiley and Sons, New York, 1984).
70. R.C. Ebewele: *Polymer Science and Technology* (CRC Press LLC, Boca Raton, 2000).
71. A. Ravve: *Principles of Polymer Chemistry*, 3rd ed. (Springer Science + Business Media, LLC, Heidelberg, 2012).
72. J.R. Fried: *Polymer Science and Technology*, 3rd ed. (Prentice Hall, Pearson Education Inc., Hoboken, 2014).
73. C.E. Carraher, Jr.: *Polymer Chemistry*, 7th ed. (CRC Press and Taylor and Francis Group, LLC, Boca Raton, 2008).
74. R.J. Young and P.A. Lovell: *Introduction to Polymers*, 2nd ed. (Chapman and Hall, Melbourne, 1991).
75. F.J. Davis, ed.: *Polymer Chemistry—A Practical Approach* (Oxford University Press, Oxford, 2004).
76. *ASM Metals Handbook*, Vol. **21** (ASM International, Materials Park, 2013).
77. T. Hong-bin and G. Cong-sheng: *Trans. Nonferrous Met. Soc. China* **21**(7), 1563–1567 (2011).
78. US Department of Defense: *Handbook of Composite Materials, Vol. 3. Polymer Matrix Composite Materials Usage, Design and Analysis* (US Department of Defense, Washington, DC, 2002).
79. G.V. Zaia: PhD thesis, Technische Universitat München, Munich, Germany (2002).
80. N. Deok-Hui, B.G. Kim, J.Y. Yoon, M.H. Lee, W-S. Seo, S-M. Jeong, C-W. Yang, and W-J. Lee: High-temperature chemical vapor deposition for SiC single crystal bulk growth using tetramethylsilane as a precursor. *Cryst. Growth Des.* **14**, 5569–5574 (2014).
81. U. Forsberg: PhD thesis, Thesis No. 708, Linköpings universitet, Linköpings, Sweden (2001).
82. US Department of Defense: *AMPTIAC Quarterly, Vol. 9, No. 2: High performance fibers for lightweight armor* (2005).
83. A.P. Mouritz: *Introduction to Aerospace Materials* (Woodhead Publishing Limited, Cambridge, 2012).


https://doi.org/10.1557/jmr.2017.63 Published online by Cambridge University Press

84. R.D. Rawlings and F.L. Matthews: *Composite Materials: Engineering and Science* (CRC Press, Woodhead Publishing Limited, Cambridge, 1999).
85. F.C. Campbell, eds: Polymer matrix composites. In *Light Weight Materials—Understanding the Basics* (ASM International, Materials Park, 2012); ch. 8.
86. A. Baker, S. Dutton, and D. Kelly: *Composite Materials for Aircraft Structures*, 2nd ed. (AIAA, Reston, 2004).
87. M. Akay: *An Introduction to Polymer Matrix Composites, 1st ed*. Ebook, www.bookboon.com.
88. K.K. Chawla: *Composite Materials—Science and Engineering*, 3rd ed. (Springer Science + Business Media, New York, 2012).
89. R-M. Wang, S-R. Zheng, and Y-P. Zheng: *Polymer Matrix Composites and Technology* (Woodhead Publishing Limited and Science Press Limited, Cambridge, 2011).
90. A. Boczkowska, S.F. Awietjan, S. Pietrzko, and K.J. Kurzydłowski: Mechanical properties of magnetorheological elastomers under shear deformation. *Composites, Part B* **43**, 636–640 (2012).
91. I. Bica, E.M. Anitas, and L.M.E. Averis: Tensions and deformations in composites based on polyurethane elastomer and magnetorheological suspension: Effects of the magnetic field. *J. Ind. Eng. Chem.* **28**, 86–90 (2015).
92. X. Qiao, X. Lu, X. Gong, T. Yang, K. Sun, and X. Chen: Effect of carbonyl iron concentration and processing conditions on the structure and properties of the thermoplastic magnetorheological elastomer composites based on poly(styrene-*b*-ethylene-*co*-butylene-*b*-styrene) (SEBS). *Polym. Test.* **47**, 51–58 (2015).
93. A. Boczkowska and S. Awietjan: Intelligent Magnetorheological elastomer composites. *Polimery* **58**(6), 443–449 (2013).
94. M. Masowski and M. Zaborski: Magnetorheological materials based on ethylene–octene elastomer. *Polimery* **59**(11–12), 825–833 (2014).
95. P. Małecki, M. Krolewicz, J. Krzak, and J. Piglowski: Dynamic mechanical analysis of magnetorheological composites containing silica-coated carbonyl iron powder. *J. Intell. Mater. Syst. Struct.* **26**(14), 1899–1905 (2015).
96. S. Aloui and M. Klüppel: Magneto-rheological response of elastomer composites with hybrid-magnetic fillers. *Smart Mater. Struct.* **24**, 025016 (2015).
97. A.M. Biller, O.V. Stolbov, and L.Y. Raikher: Mesoscopic magnetomechanical hysteresis in a magnetorheological elastomer. *Phys. Rev. E: Stat., Nonlinear, Soft Matter Phys.* **92**, 023202 (2015).
98. M.E. Nakajima and M.J.H. Heidecker: Fundamentals of polymer nanocomposites technology. In *Flame Retardant Polymer Nanocomposites*, A.B. Morgan and C.A. Wilkie, eds. (Wiley-Interscience, Hoboken, NJ, 2007).
99. E. Kandare: Development of 2-d nanostructured layered hydroxy salts (LHSs) and hydroxy double salts (HDSs) for new applications: Anionic exchange kinetics and polymer modification. PhD thesis, Marquette University, Milwaukee (2006).
100. C.J. van Oss: *Interfacial Forces in Aqueous Media* (Marcel Dekker, New York, 1994).
101. C.J. van Oss and R.J. Good: The mechanism of phase separation of polymers in organic medium-apolar and polar systems. *J. Sep. Sci. Technol.* **1**, 15–30 (1989).
102. R.A. Vaia and E.P. Giannelis: Lattice model of polymer melt intercalation in organically-modified layered silicates. *Macromolecules* **30**, 7990–7999 (1997).
103. R.A. Vaia and E.P. Giannelis: Polymer melt intercalation in organicallymodified layered silicates: Model predictions and experiment. *Macromolecules* **30**, 8000–8009 (1997).
104. A.C. Balazs, C. Singh, and E. Zhulina: Modeling the interactions between polymers and clay surfaces through self-consistent field theory. *Macromolecules* **31**, 8370–8381 (1998).
105. B. Schartel and J.H. Wendorff: Molecular composites for molecular reinforcement: A promising concept between success and failure. *Polym. Eng. Sci.* **39**(1), 128–151 (1999).
106. G. Husman, T. Helminiak, M. Wellman, W. Adams, D. Wiff, and C. Benner: Molecular composites—Rod like polymer reinforcing an amorphous polymer matrix. Technical Report, ADA086149 (Air Force Wright Aeronautical Labs, Patterson, 1980).
107. G.T. Pawlikowski, D. Dutta, and R.A. Weiss: Molecular composites and self-reinforced liquid crystalline polymer blends. *Annu. Rev. Mater. Res.* **21**, 159–184 (1991).
108. S.V. Kotomin: Polymer molecular composites—New history. *J. Thermoplast. Compos. Mater.* **26**(1), 1–18 (2011).
109. A. Millan and F. Palacio: Magnetic polymer nanocomposites. In *Polymer Nanocomposites*, Y.W. Mai and Z.Z. Yu, eds. (Woodhead Publishing Limited and CRC Press LLC, Cambridge, 2006); ch. 17.
110. S.Z.D. Cheng: *Phase Transitions in Polymers—The Role of Metastable States* (Elsevier, Amsterdam, 2008).
111. H.D. Keith: Phase transitions in high polymers. *Metall. Trans.* **4**, 2747–2754 (1973).
112. R.G. Mussati: Rheology of Network Forming Systems. PhD thesis, University of Minnesota, Minneapolis (1975).
113. M.S. Vilesova, N.P. Spasskova, L.V. Lesnevskaya, G.N. Guseva, L.G. Izrailev, and V.M. Zolotarev: *Polym. Sci. U.S.S.R.* **14**, 1883 (1972).
114. D.M. French, R.A.H. Strecker, and A.S. Tompa: The maximum extent of reaction in Gelled Systems. *J. Appl. Polym. Sci* **14**, 599–610 (1970).
115. R.S. Dave and A.C. Loos, eds.: *Processing of Composites* (Carl Hanser Verlag, Munich, 2000).
116. E. Rabinowitch: Collision Co-ordination, diffusion and reaction velocity in condensed systems. *Trans. Faraday Soc.* **33**, 1225–1233 (1937).
117. A. Saleem, L. Frormann, and A. Iqbal: Mechanical, thermal and electrical resistivity properties of thermoplastic composites filled with carbon fibers and carbon particles. *J. Polym. Res.* **14**, 121–127 (2007).
118. N.R. Roger, ed.: *Particulate-filled Polymer Composites*, 2nd ed. (Rapra Technology, Shrewsbury, 2003).
119. F.H. Gojny, M.H.G. Wichmann, B. Fiedler, W. Bauhofer, and K. Schulte: Influence of nano-modification on the mechanical and electrical properties of conventional fibre-reinforced composites. *Composites, Part A* **36**, 1525–1535 (2005).
120. R.N. Haward and G. Thackray: Use of a mathematical model to describe isothermal stress-strain curves in glassy thermoplastics. *Proc. R. Soc. London, Ser. A* **302**(1471), 453–472 (1967).
121. M.C. Boyce, D.M. Parks, and A.S. Argon: Large inelastic deformation of glassy polymers. Part 1: Rate dependent constitutive model. *Mech. Mater.* **7**, 15–33 (1988).
122. O.A. Hasan and M.C. Boyce: A constitutive model for the nonlinear viscoelastic viscoplastic behaviour of glassy polymers. *Polym. Eng. Sci.* **35**, 331–344 (1995).
123. C.P. Buckley and D.C. Jones: Glass-rubber constitutive model for amorphous polymers near the glass transition. *Polymer* **36**, 3301–3312 (1995).
124. P.J. Dooling, C.P. Buckley, and S. Hinduja: The onset of nonlinear viscoelasticity in multiaxial creep of glassy polymers: A constitutive model and its application to PMMA. *Polym. Eng. Sci.* **38**, 892–904 (1998).
125. C. Gerlach, C.P. Buckley, and D.P. Jones: Development of an integrated approach to modelling of polymer film orientation processes. *Trans. Inst. Chem. Eng., Part A* **76**, 38–44 (1998).
126. T.A. Tervoort, E.T.J. Klompen, and L.E. Govaert: A multi-mode approach to finite, three-dimensional, nonlinear viscoelastic behaviour of polymer glasses. *J. Rheol.* **40**, 779–797 (1996).


https://doi.org/10.1557/jmr.2017.63 Published online by Cambridge University Press

127. L.E. Govaert, P.H.M. Timmermans, and W.A.M. Brekelmans: The influence of intrinsic strain softening on strain localisation in polycarbonate: Modeling and experimental validation. *J. Eng. Mater. Technol.* **122**, 177–185 (2000).
128. E.T.J. Klompen, T.A.P. Engels, L.E. Govaert, and H.E.H. Meijer: Modelling of the post-yield response of glassy polymers: Influence of thermomechanical history. *Macromolecules* **38**(16), 6997–7008 (2005).
129. D.N. Theodorou and U.W. Suter: Local structure and the mechanism of response to elastic deformation in a glassy polymer. *Macromolecules* **19**(2), 379–387 (1986).
130. A.J. Kinloch and A.C. Taylor: The mechanical properties and fracture behaviour of epoxy-inorganic micro- and nano-composites. *J. Mater. Sci.* **41**(11), 3271–3297 (2006).
131. T.D. Fornes and D.R. Paul: Modelling properties of nylon 6/clay nanocomposites using composite theories. *Polymer* **44**(17), 4993–5013 (2003).
132. J-J. Luo and I.M. Daniel: Characterization and modeling of mechanical behavior of polymer/clay nanocomposites. *Compos. Sci. Technol.* **63**(11), 1607–1616 (2003).
133. J.C. Halpin and N.J. Pagano: The laminate approximation of randomly oriented fibrous composites. *J. Compos. Mater.* **3**, 720–724 (1969).
134. J.C. Halpin: Strength and expansion estimates for oriented short fibre composites. *J. Compos. Mater.* **3**, 732–734 (1969).
135. A.J. Kinloch, D.L. Maxwell, and R.J. Young: The fracture of hybrid particulate composites. *J. Mater. Sci.* **20**(11), 4169–4184 (1985).
136. B.B. Johnsen, A.J. Kinloch, R.D. Mohammed, A.C. Taylor, and S. Sprenger: Toughening mechanisms of nanoparticle modified epoxy polymers. *Polymer* **48**, 530–541 (2007).
137. K.T. Faber and A.G. Evans: Crack deflection processes—I. Theory. *Acta Metall.* **31**(4), 565–576 (1983).
138. Y. Dong, R. Umer, and A.K-T. Lau, eds.: *Fillers and Reinforcements for Advanced Nanocomposites* (Woodhead Publishing, Cambridge, 2015).
139. Q. Qin and J. Ye, eds.: *Toughening Mechanisms in Composite Materials* (Woodhead Publishing, Cambridge, 2015).
140. H. Althues, J. Henle, and S. Kaskel: Functional inorganic nanofillers for transparent polymers. *Chem. Soc. Rev.* **36**, 1454–1465 (2007).
141. A. Ghasemi, X. Liu, and A. Morisako: Effect of additional elements on the structural properties, magnetic characteristics and natural resonance frequency of strontium ferrite nanoparticles/polymer composite. *IEEE Trans. Magn.* **45**(10), 4420–4423 (2009).
142. X. Batlle, X. Obradors, J. Rodriguez-Carvajal, M. Pernet, M.V. Cabanas, and M. Vallet: Cation distribution and intrinsic magnetic properties of Co-Ti-doped M-type barium ferrite. *J. Appl. Phys.* **70**, 1614–1623 (1991).
143. K. Shimba, K. Furuta, N. Morimoto, N. Tezuka, and S. Sugimoto: Magnetic properties of nanoparticle–polymer composites prepared using surface modification and cross-linking reaction. *Mater. Trans.* **52**(3), 486–490 (2011).
144. A.P. Mouritz: Assessment of non–destructive evaluation techniques for defect detection in carbon fibre composite automotive wheels. *Proc. Inst. Mech. Eng., Part D* (2016). (under review).
145. H. Fischer: Polymer nanocomposites: From fundamental research to specific applications. *Mater. Sci. Eng., C* **23**, 763–772 (2003).

https://doi.org/10.1557/jmr.2017.63 Published online by Cambridge University Press